Single-Pion Photoproduction in a Model of Higher Baryon Couplings

Rashmi Mehrotra and A. N. Mitra
Department of Physics and Astrophysics, University of Delhi, Delhi-7, India.
(Received 23 October 1970)

Pion photoproduction off nucleons via s-channel resonances up to a total c.m. energy of ~ 2 GeV, and also the electromagnetic decay widths of such resonances, are investigated in a recently proposed unified model of $\bar{B}B_L P$ and $\bar{B}B_L V$ couplings. In this phenomenological model, which uses the "quark" language only formally, the couplings $\bar{B}B_L P$ of baryon resonance (B_L) with pseudoscalar (P) mesons in broken SU(6)$\times$O(3) are extended to incorporate electromagnetic interactions through "partial symmetry" for $\bar{B}B_L V$ couplings, together with the principle of vector-meson dominance. These supermultiplet $L^P \to 0^+$ transitions are characterized by an empirical but relativistically invariant multiplying form factor, for which two different forms are considered. The calculated electromagnetic decay widths for the baryon resonances $Y^*(1520)$ and $\Delta(1238)$ are in extremely good agreement with experiment. For the other resonances no direct experimental data are available, and comparison has been made with other contemporary analyses. The results for the reactions $\gamma p \to \pi^0 p$, $\gamma p \to \pi^+ n$, and $\gamma n \to \pi^- p$ are also presented with reference to the following types of data: (i) total cross sections, (ii) the angular distribution of the differential cross sections, (iii) the energy dependence of the cross sections at fixed angles (especially $\theta = 0$, π), and (iv) recoil-proton polarization. The agreement with the experimental data in all these respects is extremely good, thus suggesting that the direct s channel makes a large and dominant contribution to the amplitude in the intermediate-energy region. The only discrepancy lies in the forward direction for charge-exchange processes, where the t-channel pion pole is known to be important, yet a partial simulation of duality seems to be indicated by our results. Also, the qualitative features of pionic photoproduction are reasonably well reproduced by our model. The Moorhouse selection rule for spin quartet states and a "charge" selection rule proposed recently by Copley *et al.* are satisfied in the limit of $m_\rho = m_\omega$ in our model. The most prominent resonances turn out to be P_{11}, P_{33}, D_{13}, F_{15}, and F_{37}.

I. INTRODUCTION

Photoproduction of baryon resonances (B_L) represents a convenient tool for subjecting to experimental test the $\bar{B}B_L P$ and $\bar{B}B_L V$ couplings (where P and V are pseudoscalar and vector mesons, respectively) on the one hand, and the principle of vector-meson dominance (VMD) on the other. The predominantly s-channel structure of the amplitude characterizing the resonance region (1–3 GeV) disfavors the Regge mechanism and emphasizes the couplings of the $\bar{B}B_L$ currents to P and V mesons. While the idea of VMD can be given a fairly unambiguous meaning (except when some specialized polarization type of measurement is involved), the question of $\bar{B}B_L P$ and $\bar{B}B_L V$ couplings is a more model-dependent one. Some calculations on this subject have been made using a specific version of the quark model where the baryon (QQQ) wave functions are given by the nonrelativistic harmonic-oscillator model.[1-3] However, several of the interesting experimental results in these processes have had to be used as inputs for the determination of a number of crucial parameters of the model, especially the ones which bear on the $\bar{Q}\gamma Q$ interaction, so that a considerable amount of experimental material is excluded from comparison with the quantitative "predictions" of the model. We wish to present an alternative description in which it is sought to fix a considerable part of the interaction structure (and hence the associated parameters) from more theoretical considerations, so that one has a better scope for comparing the predictions of the model with experiment in a more substantial manner. We first describe the general premises and essential features of the model before proceeding with the calculational details and results.

For some time one of us (ANM) has been trying to formulate[4,5] a phenomenological model of hadron couplings to P and V mesons using for the hadron spectrum a supermultiplet representation based on SU(6)$\times$O(3). The baryons (B_L) are given by the representations $(\underline{56}, 2L^+)$ and $(\underline{70}, (2L+1)^-)$ of SU(6) $\times$O(3), together with their radial excitations.[6,7] This list is considerably smaller than the predictions of the full-fledged harmonic-oscillator model,[8,9] but seems to be more in accord with the available data.[10]

The $\bar{B}B_L P$ interactions are given by a relativistic extension of an SU(6)$\times$O(3) model which is characterized by the appearance of a relativistically invariant form factor f_L multiplying the corresponding Rarita-Schwinger interaction for an entire

supermultiplet ($L^P \to 0^+$) transition, which is more fully described elsewhere.[4,5] The $\bar{B}B_L V$ interactions are then obtained by using Schwinger's partial symmetry,[11] or broken SU(3)×SU(3) symmetry,[12] for the interaction of P and V mesons with "quark fields." This principle can be incorporated in the following expression for the (P, V) meson matrix "M" in the U(4) space of spin and isospin

$$M = i(\vec{\pi}\cdot\vec{\tau})\sigma_i q_i + i\epsilon_{ijk} q_j \sigma_i(\vec{\rho}_k\cdot\vec{\tau} + \omega_k 1) + (m_\rho \vec{\rho}_0\cdot\vec{\tau} + m_\omega \omega_0 1), \quad (1.1)$$

where the first term represents the pion coupling as generally employed in quark-model calculations, while the second and third groups of the terms generate the V-meson couplings of the "magnetic" ($\sim\sigma_i$) and "minimal" ($\sim m_{\rho,\omega}$) type, respectively. The coefficients of the various terms in M are so arranged as to reproduce the corresponding terms in the free Lagrangian with correct normalization factors when one evaluates $\frac{1}{8}\mathrm{Tr}(M^2)$. One now sees immediately that the matrix elements of M between various QQQ states would generate the necessary connections between the possible $\bar{B}B_L P$ and $\bar{B}B_L V$ couplings allowed by the quark model such that the relative magnitudes of the $\bar{B}B_L P$ and $\bar{B}B_L V$ interactions (both minimal and magnetic) are all expressible in terms of a common set of parameters characterizing, say, the $\bar{B}B_L P$ interaction.

Finally the electromagnetic interaction is simulated by the assumption of vector dominance[13] wherein the photon couples to the baryon current only via the ρ^0 or ω terms in the $\bar{B}B_L V$ interaction. Thus our model of $\bar{B}\gamma B_L$ coupling is based on the use of three distinct ingredients: (i) a quark-model coupling scheme for $\bar{B}B_L P$ in SU(6)×O(3), (ii) partial symmetry for $\bar{B}B_L V$ couplings, and (iii) VMD for electromagnetic interactions. On the other hand, calculations in a more conventional quark model[1,2] have generally been based on the assumptions (i) nonrelativistic wave functions for the baryons, especially harmonic-oscillator wave functions, and (ii) a fairly general form for the basic $\bar{Q}\gamma Q$ interaction with free parameters for the different types of terms (spin, orbital, spin-orbit, recoil, etc.). Our model therefore differs in considerable details from such quark-model calculations inasmuch as it makes use of the quark model more as a guide to the evaluation of the couplings than as a formal dynamical tool with all its implications. The real dynamics in our model resides in the form factor, which, though phenomenological in character, can be given a direct relativistic meaning without any reference to the (nonrelativistic) structure of the three-quark wave function, and whose parametrization is directly tuned to the various $B_L \to PB$ decays. Again, the partial-symmetry assumption not only eliminates the need for separate parametrizations for $\bar{B}B_L P$ and $\bar{B}B_L V$ couplings but even specifies the relative contributions of the different types (minimal and magnetic) of $\bar{B}\gamma B_L$ couplings via the VMD assumption. This hopefully eliminates a major source of ambiguity present in the more conventional quark-model treatment where the different parameters in the $\bar{Q}\gamma Q$ interaction have generally no relation to one another, and can be fixed only through important experimental constraints. Thus we are able to effect a significant reduction in the number of free parameters, and predict several experimental results which the more conventional quark model must use as input.

In this paper we shall be concerned with two types of applications of this model, viz., electromagnetic decays of baryon resonances and a detailed study of photoproduction of charged and neutral pions off both proton and neutron targets. Being interested in the main resonance region 1–2 GeV, corresponding to $L = 0, 1, 2$, we shall consider only the s-channel contributions to the various cross sections (total and differential). This assumption, which may not appear adequate at first sight because of the neglect of t-channel contributions to these processes, can nevertheless be defended on the ground that one of our primary interests is to test the duality hypothesis in at least a limited fashion. Indeed, as we shall see from the results for backward scattering (to be presented in Sec. V), the u-channel effects seem to be quite well simulated by our limited list of s-channel resonances. Similarly an analysis of the cross sections near the forward direction will be found to indicate some effect of the direct t-channel contribution, though the latter is much less quantitative than the corresponding (u-channel) effect in the backward direction. Thus a comparison of our s-channel calculation with experiment holds out the possibility of judging if, and to what extent, duality is (or is not) simulated by the addition of a fairly representative list of s-channel amplitudes. This possibility represents the main motivation for the explicit omission of the pion-pole contribution (which is of course considered by most workers) to the photoproduction amplitudes. Indeed a subtraction of our s-channel results near the forward direction from the observed cross section now provides a way of "estimating" that part of the t-channel contribution which is not simulated by our s-channel amplitude. A more ambitious test of duality could be provided by the inclusion of a further set of resonances in the 2–3-GeV region. This unfortunately has not been possible in our calculation because their experi-

mental pattern is not yet very clear, so that one needs a bigger guideline, preferably theoretical, for their collective inclusion.

Since the model has been more fully described elsewhere,[4] we shall merely record only the essential details. The calculation of photoproduction proceeds on conventional lines, except that instead of the helicity formalism, we shall find it more convenient to use the method of invariant amplitudes, which will keep us somewhat closer to the original Chew-Goldberger-Low-Nambu (CGLN) framework[14] than the language of helicity amplitudes which some recent authors[1,15] have used. Being interested in the intermediate-energy region, we shall calculate the contributions of the successive s-channel resonances N_L and Δ_L to the invariant amplitudes for the processes $\gamma p \to \pi^0 p$, $\gamma p \to \pi^+ n$, and $\gamma n \to \pi^- p$ (referred to as π^0, π^+, and π^- processes, respectively) as well as their electromagnetic decays.

In Sec. II we outline the essential features of the couplings with special reference to the form factor, for which an improved version (over the earlier parameters) has been obtained more recently.[16] Section III gives the results for the electromagnetic decays of several important resonances, strange and nonstrange, together with a comparison with numbers obtained by other methods. In Sec. IV we indicate the construction of the $\gamma N \to \pi N$ amplitudes contributed by various resonances, and write down the necessary formulas for the total and differential cross sections as well as recoil-proton polarization in terms of the appropriate invariant amplitudes which can easily be translated in terms of helicity amplitudes. Section V is devoted to a critical presentation of the numerical results in relation to the main experimental features. The fits, which turn out to be extremely good without the introduction of any free parameters, are contrasted with the results of some other recent calculations (especially the quark model) which make much greater use of free parameters to fit the data.

II. MODEL

The old $\bar{B}B_L P$ couplings which have been given elsewhere[4,5] are characterized by standard relativistic boosting of SU(6)×O(3) structures in the low-frequency limit, except for the additional prescription of $\vec{q}^2 \to -\mu^2$ for the $(L-1)$-wave terms (which are all proportional to $\vec{q}^2$). These couplings are of the two types, (I) and (II), viz.,

$$\begin{aligned} &\text{(I)}\ \ \bar{\psi}^{L+1/2}_{\mu_1\cdots\mu_L} i\gamma_5 \gamma_\mu q_\mu q_{\mu_1}\cdots q_{\mu_L}\psi, \\ &\text{(II)}\ \ m_\pi{}^2 \bar{\psi}^{L-1/2}_{\mu_2\cdots\mu_L} q_{\mu_2}\cdots q_{\mu_L}\psi \\ &\quad\text{(or } \bar{\psi}^{L+3/2}_{\mu\mu_1\cdots\mu_L} q_\mu q_{\mu_1}\cdots q_{\mu_L}\psi). \end{aligned} \tag{2.1}$$

The form factor f_L for the supermultiplet transition $L^P \to 0^+$ is given by

$$f_L = g_L \mu^{-L-1}\left(\frac{M}{m}\right)^{1/2}\left(\frac{M\mu}{-P\cdot q}\right)^{L\pm1}\left(\frac{\mu}{m_\pi}\right)^{1/2}, \tag{2.2}$$

where μ and q_μ are the mass and 4-momentum of the quantum; (M,m) are the masses of the parent and daughter hadrons, respectively; P_μ is the 4-momentum of the parent hadron; and m_π is the mass of the π meson. The indices $L\pm1$ are appropriate for decays in the corresponding partial waves. The reduced coupling constants g_L hopefully satisfy "Regge universality" for the even-L couplings, viz., $g_0 \approx g_2 \approx \cdots \approx g_{2L}$, a result which was checked for $\Delta_L \to N\pi$ decays up to $L=8$. For the odd-L couplings this was merely a conjecture. This is a simple enough scheme which not only fits the data on $B_L \to BP$ decays fairly well, but ensures the absence of otherwise free parameters, a feature which is especially desirable for the higher baryons.

More recently this parametrization has been modified[16] on the following lines. The prescription $\vec{q}^2 \to -\mu^2$ is now replaced by $\vec{q}^2 \to -m_A{}^2$, where m_A is the mass of the 1^+ meson corresponding to the P meson in the sense of partial conservation of axial-vector current (PCAC). The form factor is now given by

$$f_L = g_L\left(1, \frac{m_\pi}{m_\rho}\right)\frac{f_q}{m_\pi}\left[\sigma\left(\frac{m_A}{abc}\right)^{1/2}\right]^L\left(\frac{\mu}{m_\pi}\right)^{1/2} \tag{2.3}$$

for $L\pm1$ wave, respectively, and where σ is a scale factor adjusted from absolute decay rates to a value $\sigma = 1.8\pm0.1$. The invariants a, b, and c are given by

$$a^2 = -2P\cdot p, \quad b^2 = -2P\cdot q, \quad c^2 = -2p\cdot q, \tag{2.4}$$

where P_μ and p_μ are the 4-momenta of the parent and daughter hadrons, respectively. The dimensionless constants g_L are given by

$$g_0{}^2 \approx g_2{}^2 = \cdots = g_{2L}{}^2(?) = 1$$

and

$$g_1{}^2 \approx g_3{}^2 = \cdots = g_{2L+1}{}^2(?) \approx 0.62\pm0.1.$$

Also,

$$f_q{}^2/4\pi \approx 0.03.$$

This modification, the motivation and results of which have been described elsewhere,[16] not only turns out to give a much better fit to the $B_L \to BP$ decays, but has the following additional properties:

(i) symmetry in the momenta off the mass shell,
(ii) Regge universality for the reduced coupling constant g_L, and
(iii) explicit absence of the mass of the reso-

nance, which is now a variable quantity defined in terms of the scalar products (2.4).

We shall call the expressions (2.2) and (2.3) the "old" and "new" form factors, respectively.

The partial-symmetry principle[11] now allows us to write down the $\bar{B}BP$ and $\bar{B}BV$ couplings in a unified framework using the expression (1.1) for the M matrix, and a straightforward relativistic boosting of the resulting structures. For completeness we list the different types [(A)–(D)] of $\bar{B}BV$ couplings as

$$\begin{aligned}
&\text{(A)}\quad i\bar{\psi}\sigma_{\mu\nu}k_\mu\epsilon_\nu k_{\mu_1}\cdots k_{\mu_L}\psi^{L+1/2}_{\mu_1\cdots\mu_L}\,,\\
&\text{(B)}\quad im_V\bar{\psi}\gamma_\mu\epsilon_\mu k_{\mu_1}\cdots k_{\mu_L}\psi^{L+1/2}_{\mu_1\cdots\mu_L}\,,\\
&\text{(C)}\quad \bar{\psi}\gamma_5[ik\cdot k; m_V\gamma\cdot k]\gamma_\mu\epsilon_\mu k_{\mu_2}\cdots k_{\mu_L}\psi^{L-1/2}_{\mu_2\cdots\mu_L}\,,\\
&\text{(D)}\quad i\bar{\psi}\epsilon_{\mu\nu\lambda\sigma}k_\nu\epsilon_\lambda\gamma_\sigma k_{\mu_1}\cdots k_{\mu_L}\psi^{L+3/2}_{\mu\mu_1\cdots\mu_L}\,,
\end{aligned}\tag{2.5}$$

where k_μ and ϵ_μ are the momentum and polarization vector of the photon, respectively, and m_V is the mass of the vector meson (ρ, ω).

As to the structure of the form factors to be used for the $\bar{B}BV$ coupling, the "old" form factor [Eq. (2.2)] gives an explicit prescription, viz., the mass μ stands for the appropriate meson (P or V). This prescription has been recently used in connection with the n-p mass difference[17] with rather encouraging results. However, if we use the "new" form factor [Eq. (2.3)] as it is, it gives a factor $(m_\rho/m_\pi)^{1/2}$ too large compared to the "old" form factor even for the case $L=0$. On the other hand, we should not expect any difference between the two forms for $L=0$, and this is indeed the case for $\bar{B}BP$ couplings. As for the vector $\bar{B}BV$ coupling, the present investigation being the first example of use of the "new" form factor, we find it necessary to normalize the latter so as to agree with the "old" form factor for at least $L=0$. Therefore for use of the "new" form factor for for $\bar{B}BV$ coupling we make the following modification in the "new" form factor:

$$\frac{1}{m_\pi}\to\frac{1}{m_\rho}\left(\frac{m_\rho}{m_\pi}\right)^{1/2}=\frac{1}{(m_\rho m_\pi)^{1/2}}\,.\tag{2.6}$$

A second modification concerns the multiplying factor for the coupling of $L-\frac{1}{2}$ states, which is $(m_\pi/m_\rho)(-m_A^2)$ in the new scheme. However, for the $\bar{B}BV$ couplings of $L-\frac{1}{2}$ states such a modification is not only too *ad hoc* but does not even take care of the *two* types of (C) coupling terms given by Eq. (2.5). In this respect we believe that the simplest solution is to retain the old prescription which is more natural and has been used successfully in connection with the n-p mass difference,[17] viz., $\vec{k}^2\to -m_V^2$ and $\vec{q}^2\to-\mu^2$, where $\vec{k}^2$ appears explicitly, and to write down the straightforward relativistic extension where $\vec{k}^2$ does not appear.

The electromagnetic interaction is now included through the VMD assumption[13] which amounts to the use of the "two-point" V-γ vertex given by

$$\begin{aligned}
&\mathfrak{L}_{\text{e.m.}}=j_\mu^{\text{e.m.}}A_\mu\,,\\
&j_\mu^{\text{e.m.}}=c_\rho\rho_\mu^0+c_\omega\omega_\mu-c_\phi\phi_\mu\,,
\end{aligned}\tag{2.7}$$

where

$$c_\rho=\frac{e}{g_\rho}m_\rho^2,\quad c_\omega=\frac{e}{3g_\rho}m_\rho m_\omega,\quad c_\phi=\sqrt{2}m_\rho m_\phi\frac{e}{3g_\rho}\,,\tag{2.8}$$

and

$$\frac{g_\rho^2}{4\pi}\approx\frac{g_{\rho\pi\pi}^2}{4\pi}=\frac{1}{4\pi}G_{N\pi\pi}^2\left(\tfrac{3}{5}\right)^2=3.6\,.\tag{2.9}$$

The small ϕ term will now be omitted henceforth. As to the question of gauge invariance, it is clear that types (A) and (D) of Eq. (2.5) give rise to gauge-invariant interactions explicitly. Type (B) can be made formally gauge-invariant through the modification

$$i\gamma_\mu\epsilon_\mu\to\left(i\gamma_\mu-\frac{(P+p)_\mu}{m+M}\right)\epsilon_\mu\,.\tag{2.10}$$

Note that the second term gives a zero contribution for the process $\gamma N\to\pi N$, though its effect becomes more relevant for other processes where the photon is involved in a virtual state (e.g., in a calculation of e.m. masses). In the same way, type (C) can be seen to be gauge-invariant for a free photon. This is adequate for the present case. We should like to add that a further modification of the type (C) coupling is necessary off the photon's mass shell, but we prefer not to pursue this point here.

Before concluding this section, we give in Table I a list of the baryon resonances (together with their likely quantum numbers) to be used in our calculation. The supermultiplet classification based on the SU(6)×O(3) group accommodates most of these resonances in only two types of baryon supermultiplets, $(\underline{56}, 2L^+)$ and $(\underline{70}, (2L+1))$, where $L=0, 1, 2$ (column 2), together with their radial excitations.[7,10] The listed values of masses and total widths (column 3) for these resonances are based on a judicious observation of the Particle Data Group tables as well as more direct experimental data.[18]

In columns 4 and 5 of Table I we list the $\bar{B}BV$ and $\bar{B}BP$ couplings, respectively, which are obtained by multiplying types (A) to (D) and types (I) and (II) by (i) geometrical factors characterizing the Clebsch-Gordan expansions of the direct product of spin and orbital function and (ii) by SU(6) factors appropriate for π, ρ, and ω couplings

TABLE I. List of baryon resonances used in our calculations. For convenience we have used "pure" spin assignments (doublet and quartet indicated by d and q, respectively) for $L^P = 1^-$ resonances. Fortunately, most of the results to be discussed are not very sensitive to the mixing effect. The coupling for S_{11}^q state in our model vanishes, in conformity with the Moorhouse selection rule.

	Resonance (B_L)	L	Total width in MeV (Γ_J)	$\bar{B}\,B_L V$ coupling	$\bar{B}\,B_L P$ coupling
(1)	$N(938)$	0	...	$-A(\frac{5}{3}c_\rho\tau_3+c_\omega)+B(c_\rho\tau_3+3c_\omega)$	$\frac{5}{3}$ I
(2)	$P_{11}(1470)$	0	200	$-A(\frac{5}{3}c_\rho\tau_3+c_\omega)+B(c_\rho\tau_3+3c_\omega)$	$\frac{5}{3}$ I
(3)	$F_{15}(1690)$	2	102.0	$-A(\frac{5}{3}c_\rho\tau_3+c_\omega)+B(c_\rho\tau_3+3c_\omega)$	$\frac{5}{3}$ I
(4)	$S_{11}^d(1715)$	1	323.0	$(\frac{2}{3})^{1/2}(\frac{5}{3}c_\rho\tau_3+c_\omega)c$	$(\frac{8}{27})^{1/2}$ II
(5)	$S_{11}^q(1525)$	1	127.0	...	...
(6)	$F_{13}(1855)$	2	335.0	$(\frac{2}{5})^{1/2}(\frac{8}{3}c_\rho\tau_3+4c_\omega)c$	$\frac{1}{3}\sqrt{10}$ II
(7)	$D_{13}^d(1515)$	1	115.0	$\sqrt{2}\,[-A(\frac{2}{3}c_\rho\tau_3+c_\omega)+c_\rho\tau_3 B]$	$\frac{2}{3}\sqrt{2}$ I
(8)	$D_{13}^q(1675)$	1	101.0	$(\frac{2}{15})^{1/2}(c_\rho\tau_3-3c_\omega)A$	$-(\frac{2}{15})^{1/2}$ I
(9)	$D_{15}^q(1675)$	1	238.0	$(\frac{1}{3})^{1/2}(c_\rho\tau_3-3c_\omega)D$	$(\frac{1}{3})^{1/2}$ II
(10)	$P_{33}(1238)$	0	101.0	$4(\frac{1}{3})^{1/2}c_\rho D$	$-(\frac{8}{3})^{1/2}$ II
(11)	$F_{37}(1940)$	2	245.0	$4(\frac{1}{3})^{1/2}c_\rho D$	$-(\frac{8}{3})^{1/2}$ II
(12)	$S_{31}^d(1630)$	1	160.0	$-(\frac{8}{27})^{1/2}c_\rho c$	$\frac{1}{3}(\frac{1}{3})^{1/2}$ II
(13)	$D_{33}^d(1670)$	1	225.0	$-\sqrt{2}\,c_\rho(\frac{1}{3}A+B)$	$\frac{1}{3}$ I
(14)	$F_{35}(1880)$	2	250.0	$(\frac{1}{7})^{1/2}Ac_\rho$	$(\frac{8}{7})^{1/2}$ I

to the $\bar{B}B_L$ currents. Finally for the case of pion production the appropriate charge structures are taken care of through the following SU(2) isospin factors associated with $\bar{B}B_L P$ couplings: factors 1, $\sqrt{2}$, and $\sqrt{2}$ ($I=\frac{1}{2}$) and $-\sqrt{2}$, 1, and -1 ($I=\frac{3}{2}$) for the π^0, π^+, and π^- processes, respectively. Here, a factor $-1/\sqrt{3}$ is already included in the last column of Table I. For γ coupling the complete SU(2) isospin structure is displayed in Table I.

III. ELECTROMAGNETIC DECAY WIDTHS

The electromagnetic decays of baryon resonances are not of as direct physical interest as their photoproduction cross sections, but a study of the relative magnitudes of the former should nevertheless provide a sufficient indication of the photoproduction rates of these resonances. Since these decay widths are extremely small quantities, little direct experimental guidance is available on these numbers, and the effective "data" for comparison are (i) the results of multipole analyses of pion photoproduction[19] and (ii) the e.m. decay predictions of the harmonic-oscillator quark model.[1-3] In respect of the latter it is important to keep in mind that while in the quark model the input values to be used for several important parameters in the basic $\bar{Q}\gamma Q$ coupling must be fixed from experiment, the present model specifies uniquely (via the partial-symmetry principle) the relative coupling strengths of the different types of (magnetic, minimal, etc.) interaction so that our predictions are much more specific than, e.g., those of CKO.[1]

The amplitude M_γ for a typical process $N^* \to N\gamma$

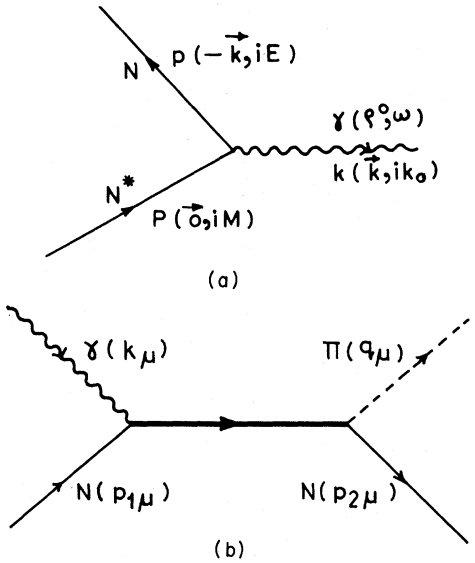

FIG. 1. (a) Electromagnetic decay of baryon resonances. (b) Feynman diagram for the process $\gamma N \to \pi N$ in s channel.

for the resonances listed in Table I is given by [see Fig. 1(a)]

$$M_\gamma = f_L^V(k^2) V_{N^* N\gamma} . \tag{3.1}$$

Here $f_L^V(k^2)$ is the supermultiplet form factors given by Eqs. (2.2) and (2.3), and $V_{N^* N\gamma}$ represents the appropriate coupling structures [types (A) to (D) together with SU(6) Clebsch-Gordan factors] which are listed in the fourth column of Table I. The electromagnetic decay width can now be written as

$$\Gamma = \frac{1}{2J+1} \frac{mk}{2\pi M} \sum_{\text{spin}} |M_\gamma|^2 , \tag{3.2}$$

where M is the mass of the decaying resonance, m that of the final nucleon, and k the energy of the photon.

Table II lists the calculated decay widths for the processes $N^{*+} \to p\gamma$ and $N^{*0} \to n\gamma$ for a few typical states of $(\underline{70}, 1^-)$ and $(\underline{56}, 0^+)$ and $(\underline{56}, 2^+)$ baryons using "old" and "new" form factors. The magnetic ($M1$) and electric ($E2$) modes for the more important states like P_{11}, F_{15}, D_{13}, and D_{33} are listed separately to bring out the relative strengths of the $M1$ and $E2$ transitions in their photoproduction cross sections.

The Moorhouse selection rule,[20] which is also supported by experiment,[21] states that in a quark model

$$\Gamma(D_{15}^+ \to p\gamma) = 0, \tag{3.3}$$

but

$$\Gamma(D_{15}^0 \to n\gamma) \neq 0. \tag{3.4}$$

This is a consequence of the vanishing of the matrix element of the magnetic term in the $\bar{Q}\gamma Q$ coupling between a charged initial state of $S = \frac{3}{2}$ and a $p\gamma$ final state. Note that for the electromagnetic transition of an $S = \frac{3}{2}$ state only the magnetic (spin-flip) part of the $\bar{Q}\gamma Q$ coupling (and *not* its electric part) contributes. In our model of vector dominance (VMD) the charged decay of the state $D_{15}(1675)$, although extremely small ($\sim 10^{-4}$, see Table II), reduces to zero only in the limit of $m_\rho = m_\omega$. Thus the (small) difference of the ρ and ω masses violates the Moorhouse selection rule in VMD. Indeed, the limit $m_\rho = m_\omega$, which in the VMD model signifies exact cancellation between the ρ and ω contributions to the electromagnetic coupling of a proton-like resonance, corresponds in the quark model to the assumption of "normal" magnetic moments of the "proton" and "neutron" quarks, and this last represents the essential clue to an understanding of the Moorhouse rule. On the other hand, the zero width for the decay of an S_{11}^q state to $N + \gamma$ does not even depend on the cancellation between the ρ and ω contributions to the electromagnetic coupling, since these contributions are now separately zero so that the transition $S_{11}^q \to N\gamma$ is forbidden for both protonlike and neutronlike states. The case of D_{13}^q is similar to that of D_{15}^q rather than the S_{11}^q state. The transitions from the charged quartet states D_{15}^q and D_{13}^q are at least four orders of magnitude smaller than those from the corresponding doublet states but reduce to zero only when the masses of ρ and ω are taken to be same. The decays of D_{15}^q and D_{13}^q to the corresponding neutral states on the other hand are quite appreciable (see Table II), for the reasons stated above.

A similar aspect of our VMD model is also noticeable in the neutral decay of some of the $(\underline{56}, L^+)$ states, viz., $P_{11}(1470)$ and $F_{15}(1690)$, via the "minimal" electromagnetic term. Only in the limit of $m_\rho = m_\omega$ is the "minimal" term proportional to $\frac{1}{2}(1 + \tau_3)$, and hence it gives vanishing contribution for the transition $N^{*0} \to n\gamma$. This result is completely equivalent to the "charge" selection rule of CKO valid for $\underline{56}$ states of $I = \frac{1}{2}$. However, a consideration of the actual (unequal) masses of ρ and ω leads to a finite (though extremely small) violation of this rule. [On the other hand, the "minimal" couplings of $\underline{70}$ states have a charge structure which is quite different from the $\frac{1}{2}(1 + \tau_3)$ dependence valid for $\underline{56}$ states.] Both the Moorhouse and CKO selection rules are discussed in greater detail in Sec. V, in connection with photoproduction data.

For a more quantitative discussion of electromagnetic decay widths we first note that the only radiative decays for which we have direct experimental evidence are $P_{33}(1238) \to N\gamma$ and $Y^*(1520) \to \Lambda\gamma$, whose measured values are 0.65 MeV (Ref. 22) and 0.15 ± 0.03 MeV (Ref. 23), respectively. Our calculated values for $P_{33} \to N\gamma$ are 0.528 and 0.697 MeV with the "new" and "old" form factors (2.3) and (2.2), respectively; the lower value obtained with the "new" form factor being merely the result of dropping the factor $(M/m)^{1/2}$ in the "old" coupling structure.[16] For the singlet resonance $Y^*(1520)$ we obtain similarly the values 0.106 and 7.824 MeV with the "new" and "old" form factors, respectively. Thus for this case the prediction of the "new" form factor is far better than that of the "old". For the case of $Y^*(1405) \to \Lambda\gamma$, which is still awaiting measurement, our "old" and "new" predictions are 0.0075 and 0.0381 MeV, to be compared with CKO's value of 0.157 MeV.

For the electromagnetic decays of other resonances which are listed in Table II no direct experimental data are available for comparison, so this table has been designed to bring out merely two types of comparison: (i) one between the pre-

TABLE II. The electromagnetic decay widths of baryon resonances in MeV. θ_S and θ_D are the mixing angles which measure the "tilt" from the doublet states, their values in terms of Ref. 2 being 35°, and 35° or 127°, respectively. The neutral and charged decay rates of the Δ state are, of course, the same.

		$\Gamma\ (B_L^+ \to p\gamma)$			$\Gamma\ (B_L^0 \to n\gamma)$		
	Resonance (B_L)	"Old" form factor	"New" form factor	Other experimental and theoretical results	"Old" form factor	"New" form factor	Other experimental and theoretical results
(1)	P_{11}	1.154 0.116	0.739 0.074	0.13[a] 0.39 or 0.43[b]	0.527 0.213×10^{-4}	0.336 0.136×10^{-4}	0.05[a]
(2)	$S_{11}(1715)$	$3.3\sin^2\theta_S$	$0.151\sin^2\theta_S$	0.4[a]	$1.504\sin^2\theta_S$	$0.069\sin^2\theta_S$	0.11[a]
(3)	$D_{13}(1515)$	$(1.839\cos\theta_D$ $-0.012\sin\theta_D)^2$	$(0.192\cos\theta_D$ $-0.002\sin\theta_D)^2$	0.35 or 0.2[a] 0.22[b]	$(0.817\cos\theta_D$ $-0.902\sin\theta_D)^2$	$(0.085\cos\theta_D$ $-0.094\sin\theta_D)^2$	0.14[a]
(4)	$D_{13}(1675)$	$(2.133\sin\theta_D$ $+0.014\cos\theta_D)^2$	$(0.265\sin\theta_D$ $+0.0018\cos\theta_D)^2$	0.36 or 0.7[a]	$(0.928\sin\theta_D$ $+1.053\cos\theta_D)^2$	$(0.115\sin\theta_D$ $+0.13\cos\theta_D)^2$	0.25[a]
(5)	D_{15}	0.186×10^{-3}	0.029×10^{-4}	0.0[c]	1.021	0.016	0.2[a]
(6)	F_{13}	0.91	0.051	...	0.111	0.006	...
(7)	F_{15}	0.992 0.084	0.028 0.003	0.26[a]	0.451 0.153×10^{-4}	0.013 0.043×10^{-5}	0.11[a]
(8)	P_{33}	0.697	0.528	0.65[d]			
(9)	S_{31}	1.754	0.102	0.1[a]			
(10)	D_{33}	0.47 0.359	0.008 0.006	0.13[a]			
(11)	F_{35}	0.768	0.028				
(12)	F_{37}	0.716	0.0276	0.23[a]			

[a]Reference 2. [b]Reference 19. [c]Reference 20. [d]Reference 22.

dictions of the "old" and "new" form factors and (ii) a second with the results of Refs. 2, 19, 20, and 22. Our model which of course conforms to both the Moorhouse and CKO selection rules seems to give uniformly large magnitudes in terms of the "old" form factor but moderate numbers when calculated with the "new" form factor.

For a comparison of our results with other calculations[1,19] we note that the CKO prediction of much stronger coupling of $F_{15}(1688)$ resonance to protons than to neutrons is also borne out by our model. Indeed while the electric transitions to $p\gamma$ and $n\gamma$ states are in the ratio of $\sim 10^4$ (cf. "charge" selection rule of CKO) even the magnetic transitions to these states are in the ratio $\gtrsim 2:1$, as may be seen from Table II. This fact seems to be indirectly confirmed through a recent experiment on photoproduction of this resonance. Another interesting result is that the charged decay rate of the $P_{11}(1470)$ resonance is about twice as high as the neutral decay rate. This mechanism is exactly similar to the case of F_{15} in view of the generally accepted assignment of the $P_{11}(1470)$ to a radially excited state of $\underline{56}$,[9,10] and gives almost the opposite prediction to that of the $\overline{10}$ representation for this resonance,[24,25] an idea which is now regarded as obsolete. Again, for the case of the D_{13} resonance, the charged decay rate is seen to be higher than the corresponding neutral decay rate, in full agreement with the harmonic-oscillator model.[2]

On the whole, our decay predictions calculated with the "new" form factor overlap fairly well with the results of Refs. 2 and 19, but the numbers obtained with the "old" form factor are appreciably higher.

IV. FORMALISM FOR PHOTOPRODUCTION

To calculate the amplitude for the process $\gamma N \to \pi N$ via s-channel resonances (N and Δ type) let the four-momenta of the initial and final nucleons be $p_{1\mu} = (-\vec{k}, iE_1)$ and $p_{2\mu} = (-\vec{q}, iE_2)$, respectively, and those of the (initial) photon (polarization ϵ_μ) and (final) pion be $k_\mu = (\vec{k}, ik_0)$ and $q_\mu = (\vec{q}, \omega_q)$, respectively [see Fig. 1(b)]. The following symbols establish the notations for the various kinematical quantities used in the calculation, in the pion-nucleon center-of-mass system:

$$\begin{aligned} s &= -(k+p_1)^2 = W^2 , \\ t &= -(k-q)^2 = m_\pi^2 + 2(|\vec{k}|\,|\vec{q}|\cos\theta - k_0\omega_q) , \\ u &= -(k-p_2)^2 = m^2 - 2(|\vec{k}|\,|\vec{q}|\cos\theta + k_0 E_2) , \end{aligned} \tag{4.1}$$

where θ is the s-channel c.m. angle between $\vec{q}$ and $\vec{k}$; the metric used is $A\cdot B \equiv A_\mu B_\mu = \vec{A}\cdot\vec{B} - A_0 B_0$, $q^2 = -m_\pi^2$, and $p_1^2 = p_2^2 = -m^2$.

In the center-of-mass system we have the following simplifications:

$$\begin{aligned} &P_\mu = (k+p_1)_\mu = (q+p_2)_\mu = (\vec{0}, iW) , \\ &P\cdot\epsilon = 0, \quad p_1\cdot\epsilon = -k\cdot\epsilon = 0 , \\ &q\cdot\epsilon = -p_2\cdot\epsilon \neq 0 . \end{aligned} \tag{4.2}$$

The amplitude for the process $\gamma N \to \pi N$ via an s-channel resonance of spin $l+\frac{1}{2}$, mass M, and four-momentum P_μ is now given by

$$F_{l+1/2} = 2V_\gamma M \Theta(l+\tfrac{1}{2}, P) V_\pi / (P^2 + M^2) , \tag{4.3}$$

where V_γ and V_π are the vertices arising from $\gamma N^* N$ and $\pi N^* N$ interactions, respectively, described in Sec. II, and $\Theta(l+\frac{1}{2})$ is the off-shell projection operator for the N^* state[26]

$$\Theta^{(\nu)}_{(\mu)}(l+\tfrac{1}{2}) = \frac{l+1}{2l+3}\gamma_\mu\gamma_\nu\Theta^{\nu\nu_1\cdots\nu_l}_{\mu\mu_1\cdots\mu_l}(l+1)\frac{M - i\gamma_\mu P_\mu}{2M} . \tag{4.4}$$

The projection operator $\Theta(l+1)$, in turn, is that of a "boson" of spin $(l+1)$ off the mass shell. The reduction of (4.4) is achieved through the use of the following relations[26]:

$$q_\mu q_{\mu_1}\cdots q_{\mu_l}\Theta^{(\nu)}_{(\mu)}(l+1)k_\nu k_{\nu_1}\cdots k_{\nu_l} = \frac{2l+3}{p(l+1)}(\bar{q})^{l+1}(\bar{k})^{l+1}P_{l+1}(\bar{z}) \tag{4.5}$$

and

$$V_\mu q_{\mu_1}\cdots q_{\mu_l} = \frac{1}{l+1}\left(V\cdot\frac{\partial}{\partial q}\right) q_\mu q_{\mu_1}\cdots q_{\mu_l} , \tag{4.6}$$

where V_μ is a vector standing for P_μ, ϵ_μ, or γ_μ, and

$$\bar{q}^2 = q\cdot\Theta\cdot q, \quad \bar{k}^2 = k\cdot\Theta\cdot k, \quad \bar{z} = q\cdot\Theta\cdot k/\bar{q}\bar{k} , \tag{4.7}$$

$$p(l+1) = \Gamma(2l+4)/[2^{l+1}\Gamma^2(l+2)] , \tag{4.8}$$

$$A\cdot\Theta\cdot B = A_\mu\Theta^\nu_\mu B_\nu , \tag{4.9}$$

$$\Theta^\nu_\mu = \delta_{\mu\nu} + P_\mu P_\nu / M^2 . \tag{4.10}$$

The total s-channel amplitude is obtained by summing the contributions of the type (4.3) for the entire catalog of resonances listed in Table I. It is now convenient to express the total amplitude $\sum_J$ in terms of four invariant amplitudes A_1–A_4 taking account of the relations (4.2) which are valid in the c.m. frame:

$$M_{\pi\gamma} = \bar{u}(p_2)\gamma_5(A_1 i\gamma\cdot\epsilon + A_2\gamma\cdot k\gamma\cdot\epsilon + iA_3 q\cdot\epsilon\gamma\cdot k + A_4 q\cdot\epsilon)u(p_1) . \tag{4.11}$$

The coefficients A_i ($i = 1$–4) can easily be expressed in terms of the contributions of the vari-

ous resonances according to Eqs. (4.5)–(4.10).

The differential cross section is given by

$$\frac{d\sigma}{d\Omega}=\sum \frac{m^2}{16\pi^2 W^2}\frac{|\vec{q}|}{|\vec{k}|}|M_{\pi\gamma}|^2, \tag{4.12}$$

where $\sum$ denotes the appropriate sum and average over the final and initial spins, respectively.

For the polarization structure of the amplitude, it is possible to consider two types of effects: (i) the asymmetry arising from the polarized photons, and (ii) the polarization of the recoil proton using an unpolarized photon beam. In our model of vector dominance, the former effect essentially reflects on the polarization structure of the vector meson (ρ or ω) to which the photon is coupled. Since in the following paper[27] dealing with an application of this coupling scheme to the process $\pi N \to (\rho, \omega)N$ the structure of the various density-matrix elements is studied in detail, we prefer not to duplicate, in this paper, this aspect of the polarization problem, and concentrate merely on the complementary problem of recoil-proton polarization. This quantity is most easily obtained in terms of the standard four-dimensional operations on the squared modulus of (4.11) except for not summing over the polarization of the final nucleon. Thus the result of averaging over the initial spin can be expressed as

$$\langle |M_{\pi\gamma}|^2\rangle_{\text{average}}=\bar{u}(p_2)X\cdot\epsilon\frac{m-i\gamma\cdot p_1}{2m}\gamma_4 X^\dagger\cdot\epsilon^*\gamma_4 u(p_2), \tag{4.13}$$

where

$$\epsilon\cdot X=\gamma_5(A_1 i\gamma\cdot\epsilon+A_2\gamma\cdot k\gamma\cdot\epsilon+iA_3 q\cdot\epsilon\gamma\cdot k+A_4 q\cdot\epsilon) \tag{4.14}$$

and

$$u(p_2)=\frac{m-i\gamma\cdot p_2}{[2m(E_2+m)]^{1/2}}u(0). \tag{4.15}$$

Averaging over the initial photon polarizations leads eventually to the three-dimensional structure of the form

$$\bar{u}(0)[(\mathrm{RE})+(\vec{\sigma}\cdot\hat{n})|\vec{k}||\vec{q}|\sin\theta(\mathrm{IM})]u(0) \tag{4.16}$$

from which the magnitude of the polarization vector (which is necessarily parallel to $\hat{n}$) is deduced as

$$|\vec{P}|=|\vec{k}||\vec{q}|\sin\theta(\mathrm{IM}/\mathrm{RE}), \tag{4.17}$$

where

$$\begin{aligned}\mathrm{RE}=\frac{1}{2m^2}&(|A_1|^2(m^2+E_1E_2-\vec{q}\cdot\vec{k})+2k_0^2W(E_2+|\vec{q}|\cos\theta)(|A_2|^2+\tfrac{1}{2}\vec{q}^2\sin^2\theta|A_3|^2)\\&-mk_0\times2(E_2+W+|\vec{q}|\cos\theta)\,\mathrm{Re}(A_1^+A_2)\\&+\tfrac{1}{2}\vec{q}^2\sin^2\theta\{2mk_0(\omega_q-|\vec{q}|\cos\theta)\mathrm{Re}(A_3^+A_4)-(A_4)^2(m^2-E_1E_2+\vec{q}\cdot\vec{k})\\&-2m\,\mathrm{Re}(A_1^+A_4)+2k_0W[\mathrm{Re}(A_1^+A_3)+\mathrm{Re}(A_2^+A_4)]\}\end{aligned} \tag{4.18}$$

and

$$\begin{aligned}\mathrm{IM}=&-\frac{W}{m^2}(\mathrm{Im}A_1^+A_2+\tfrac{1}{2}\vec{q}^2\sin^2\theta\,\mathrm{Im}A_3^+A_4)+\frac{\mathrm{Im}A_1^+A_4}{2m}\left(-\frac{E_2}{m}+\frac{E_1}{m}\frac{|\vec{q}|\cos\theta}{k_0}\right)\\&-(E_2+|\vec{q}|\cos\theta)\left(\frac{\mathrm{Im}A_1^+A_3}{2m}+\frac{\mathrm{Im}A_2^+A_4}{2m}-\frac{Wk_0}{m^2}\mathrm{Im}A_2^+A_3\right)+W\left(\frac{\mathrm{Im}A_2^+A_4}{2m}-\frac{\mathrm{Im}A_1^+A_3}{2m}\right).\end{aligned} \tag{4.19}$$

Here, the RE part in Eq. (4.18) is proportional to the unpolarized differential cross section (4.12).

To illustrate the calculations and to specify our normalization for the amplitudes A_i, we evaluate the contribution from a typical resonance of $J=L+\frac{1}{2}$ for the case of couplings of type (A) of Eq. (2.5) and type (I) of Eq. (2.1) for the $\bar{B}BB_LV$ and $\bar{B}BB_LP$ vertices, respectively. The amplitude for this case is

$$F^{L+1/2}=f_L^M(q^2)f_L^V(k^2)C_\pi C_\gamma M_{\pi\gamma}/(P^2+M^2), \tag{4.20}$$

where $f_L^M(q^2)$ and $f_L^V(k^2)$ are the supermultiplet form factors for the BB_LP and BB_LV vertices, respectively, and C_γ and C_π are the appropriate geometrical factors (which are independent of momentum) and can be directly read from the last two columns of Table I. The factor $M_{\pi\gamma}$ is given by

$$M_{\pi\gamma}=\bar{u}(p_2)i\gamma_5\gamma\cdot q\,q_{\nu_1}\cdots q_{\nu_l}\Theta^{\nu\nu_1}_{\mu_1\mu_2}\cdots{}^{\nu_l}_{\mu_L}(L+\tfrac{1}{2})k_{\mu_1}k_{\mu_2}\cdots k_{\mu_L}\sigma_{\mu\nu}k_\mu\epsilon_\nu u(p_1), \tag{4.21}$$

which simplifies on the use of Eqs. (4.5)–(4.10) to

$$M_{\pi\gamma}=\frac{1}{[p(L+1)](L+1)}\bar{u}(p_2)i\gamma_5\gamma\cdot q\left(\gamma\cdot\frac{\partial}{\partial q}\right)(\bar{q}_\nu)^{L+1}P_{L+1}(\bar{z})(\bar{k}_\mu)^{L+1}\left(\gamma\cdot\frac{\partial}{\partial k}\right)(M-i\gamma\cdot P)\sigma_{\mu\nu}k_\mu\epsilon_\nu u(p_1). \tag{4.22}$$

To extract the coefficients to the invariants A_1 to A_4 of Eq. (4.22) it is convenient to write down the expansion of the Legendre function and to carry out the differentiation in a straightforward way. From the resulting expression the individual coefficients are easily identified as

$$A_1 = \frac{c_f}{2^{L+1}(L+1)p(L+1)} \sum_{n=0}^{E(L+1)/2} \frac{(-1)^n (2L-2n+2)!}{n!(L+1-2n)!(L+1-n)!} z^{L-2n-1} \bar{k}^{2n-2} \bar{q}^{2n-2} \times 2P\cdot k \left\{ (m+M)a + \left[2z(m+M) + \frac{P\cdot k m_\pi^2}{M} + \frac{P\cdot k P\cdot q}{M^2}\left(2M + \frac{P^2}{M^2}(m+M)\right)\right] b \right\}, \tag{4.23}$$

$$A_2 = \frac{c_f}{2^{L+1}(L+1)p(L+1)} \sum_{n=0}^{E(L+1)/2} \frac{(-1)^n (2L-2n+2)!}{n!(L+1-n)!(L+1-2n)!} z^{L-2n-1} \bar{q}^{2n-2} \bar{k}^{2n-2} \times \left\{ a\eta + \left[2z\eta + m_\pi^2 P\cdot k \left(2 + \frac{P^2}{M^2} - \frac{m}{M}\right) - \frac{q\cdot P P\cdot k}{M}\left(4mM - \frac{P^2}{M^2}\eta\right)\right] b \right\}, \tag{4.24}$$

$$A_3 = 0.0, \tag{4.25}$$

and

$$A_4 = 0.0, \tag{4.26}$$

where the summation is to be done for $n = \frac{1}{2}(L+1)$ and $\frac{1}{2}L$ if $L+1$ is even or odd, respectively, and

$$\eta = P^2 - 2mM - m^2, \tag{4.27}$$

$$a = (L+1-2n)z[2n\bar{k}^2 q_P\cdot q_P + 2n\bar{q}^2 k_P\cdot k_P + 8n^2 z^2 q_P\cdot k_P + (4 + P^2/M^2)\bar{k}^2\bar{q}^2], \tag{4.28}$$

$$b = (L+1-2n)(L-2n)\bar{q}^2\bar{k}^2 - 4n^2 z^2, \tag{4.29}$$

and

$$x_P = x_\mu + \frac{x\cdot P P_\mu}{M^2} \qquad (x = q \text{ or } k). \tag{4.30}$$

The quantity c_f specifies the other factors apart from $M_{\pi\gamma}$ in Eq. (4.20). Finally, for the propagator $1/(P^2+M^2)$ we take $M \to M - i\Gamma_J/2$ where Γ_J is the total resonance width indicated in column 2 of Table I.

Contributions to A_i from the other resonances as well as other types of $\bar{B}BB_L V$ and $\bar{B}BB_L P$ couplings can easily be identified on similar lines.

V. RESULTS AND DISCUSSION

For a discussion of the numerical results for photoproduction in the resonance region, it is convenient to keep in mind the main experimental features bearing on (i) the angular distribution, especially the resonance characteristics in the forward and backward directions, and (ii) the energy dependence of the total cross sections. Some experimental features,[1,15,19,21,28,29] which are generally recognized, are: (a) Certain resonances, e.g., $D_{13}(1515)$ and $F_{15}(1680)$, which contribute strongly to the total cross sections do not show up in the forward and backward directions. (b) In the backward direction ($\theta = \pi$) several of the $I = \frac{3}{2}$ resonances only are prominent over a wide energy range. (c) Certain low-J-spin resonances are difficult to discover in the curves for the cross sections. (d) In the forward direction the cross sections for the charge-exchange reactions $\gamma p \to \pi^+ n$ and $\gamma n \to \pi^- p$ are about 12 times larger than for $\gamma p \to \pi^0 p$ (non-charge-exchange).

A. t-channel Effects

Let us first dispose of the last feature (d) above, in terms of a short discussion on the t-channel effects. The present model, which is based entirely on the effect of s-channel contributions of the various resonances, cannot of course be expected to account for the t-channel effects whose most important manifestation lies in pion exchange. Thus for photoproduction off protons, the model would be fairly adequate for π^0 production, which receives no contribution from pion exchange, but not for π^+ production, which is expected to receive a substantial contribution from it especially near the forward direction.[15,19] Therefore in our model the ratio of π^+ to π^0 amplitudes would reflect merely on the effect of Clebsch-Gordan coefficients, and not the extra contribution which arises from pion exchange in the π^+ case. On the other hand, if duality holds in a broad sense, one would expect the t-channel effects to be at least partly simulated through the addition of a fairly extensive list of s-channel resonances. Thus a comparison of the ratio of

the π^+ to π^0 cross sections at $t=0$ should provide some qualitative idea of the duality effect, after taking account of the isospin Clebsch-Gordan coefficients which make the amplitude ratios for π^+ to π^0 production $\sqrt{2}$ and $-1/\sqrt{2}$ for the contributions from $I=\frac{1}{2}$ and $I=\frac{3}{2}$ resonances, respectively. A look at Figs. 4, 5, 6, and 7 (to be discussed more fully later) already shows that near the forward direction the ratios of these differential cross sections ~3, which, while falling far short of the experimental value ($\gtrsim 10$), is nevertheless appreciably larger than what one would expect of Clebsch-Gordan coefficients alone, even taking account of unequal interference from the various resonances to the two cross sections. It is tempting to interpret this "surplus" over Clebsch-Gordan effects as indicating some sort of effect of duality which is presumably simulated even through our limited list of resonances. On the other hand, the magnitude of the effect would seem to indicate that our limited list of s-channel resonances fail to produce the full effect of the direct t-channel contribution. It may be noted, however, that the effect of our omission of the t channel is much less pronounced at nonforward directions so that we may expect our s-channel contributions alone to provide the dominant mechanism for photoproduction at intermediate energies at all but the near forward directions. We now turn to the other items (a)–(c) of our listed experimental features, keeping this general limitation of our model in mind.

B. Total Cross Section (σ_T)

While the best test of the individual s-channel contributions of the various resonances to the total cross section (σ_T) is provided by a comprehensive partial wave analysis, e.g., of the type given in Ref. 15, it is nevertheless possible to obtain a fairly good idea of the effect of the more important contributors amongst the resonances from an examination of σ_T as a function of energy. The theoretical σ_T curves which were obtained by integrating Eq. (4.12) in a straightforward manner over the complete solid angle with both the "old" and "new" form factors are shown in Figs. 2, 3(a), and 3(b) as functions of photon energy in the lab system (E_γ). The solid and dashed curves represent the "new" and "old" form factors, respectively. Specifically, the cases of π^+ and π^- have been treated with the "old" and "new" form factors, respectively, while for π^0 the effects of both form factors have been included for a comparison. As these π^0 curves in Fig. 1 indicate, the difference between the predictions of the old and new form factors for this case is rather small, so that the

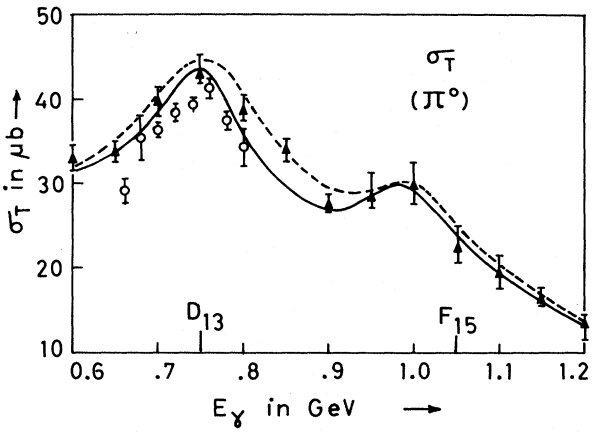

FIG. 2. Total cross section (σ_T) in μb with "old" (dashed curve) and "new" (solid curve) form factors for the process $\gamma p \to \pi^0 p$ as a function of lab photon energy E_γ in GeV compared with the data of (▲) Ref. 30 and (○) Ref. 31.

σ_T data do not seem to be very sensitive to the difference between the two. As to the experimental points, they were obtained from Refs. 30 to 39, where the σ_T's were obtained from the respective data on the differential cross sections after fitting the latter to polynomials of varying degrees and then integrating the resulting functions over the complete solid angle.

An examination of the Figs. 1, 2, and 3 shows that the theoretical curves indeed fit the experimental points excellently, for both types of form factors. The effect of t-channel exchanges on σ_T does not appear to be important since the s-channel curves for π^+ and π^- overlap considerably with the corresponding experimental points. This is not unreasonable since the pion-exchange contribution falls off rapidly beyond $t=0$, so that its over-all contribution to σ_T is probably not large. Several resonances, especially P_{33}, D_{13}, F_{15}, stand out prominently, in full accord with experiment. For several other resonances, however, their individual effects do not seem to be marked. Presumably, these resonances contribute collectively to make an over-all quantitative effect, partly overlapping with the contributions of the more prominent resonances. Thus, e.g., the peak near the c.m. energy $W=1.5$ GeV can at least partly be ascribed to the effect of the $P_{11}(1470)$ resonance. Similarly, the peak near $W=1.65$ GeV in π^- is partly due to D_{33} and the spin quartet resonances D_{15}^q and D_{13}^q. On the other hand, for the processes π^0 and π^+, only the D_{33} makes a partial contribution to the peak near $W=1.65$ GeV, while the spin quartet resonances D_{15}^q and D_{13}^q do not make any contribution because of the cancellation of the ρ

and ω contributions to the electromagnetic coupling of protons (see Sec. III). The effect of F_{37} is also visible in the theoretical and experimental curves, though not so prominently as some others. Finally, the effect of relatively low-J resonances such as S_{11} and S_{31} have been numerically found to be so small ($\sim\frac{1}{10}$th of the contribution of their immediate high-J neighbors) that it is hardly surprising that they do not show up in σ_T (in spite of their appreciable electromagnetic decay widths). A similar argument applies also to $F_{13}(1860)$, whose proximity to the $F_{37}(1940)$ peak, which has a much larger J value, makes it difficult to distinguish in that energy region. These results on relatively low-J resonance are in general accord with experiment [cf. feature (c)], though not with the results of CKO,[1] who find an appreciable contribution of S_{11} and S_{31} to σ_T.

The σ_T curves for π^+ and π^- are similar, but the peaks of the latter are much less pronounced than those of π^+, especially for F_{15}. This is a manifestation of cancellation between the isoscalar and isovector parts of the "minimal" electromagnetic term in γn coupling and their reinforcement in γp coupling in agreement with the selection rule of CKO. However, the much smaller accuracy for π^- data compared with π^+ does not warrant a strong conclusion on this point. We shall discuss this point again in connection with differential cross sections.

C. Energy and Angular Dependence of Differential Cross Section

To get a better insight into the contributions of the different resonances to photoproduction we now analyze the results for the differential cross sections as functions of (i) angles at fixed energies and (ii) energies at fixed angles. It is convenient to discuss the cases of π^0, π^+, and π^- production separately for both types of analyses.

Figures 4, 5, and 6 show the angular distribution for the three cases at the indicated lab photon energies E_γ in GeV which have been chosen to cover all the resonances up to ~2 GeV. The angular distribution for π^0 (Fig. 4) seems to be in extremely good agreement with experiment (Refs. 40 to 48) at all the energies indicated. The characteristic feature above 1 GeV is a pronounced peak in the forward direction which moves to smaller angles as energy increases. At $E_\gamma = 1.175$ GeV this peak occurs at $\theta \approx 40°$ and is well reproduced by our model, demonstrating once again that the s-channel resonances are adequate to describe this process. At $E_\gamma = 0.7$ and 0.8 GeV [Figs. 4(d) and 4(c), respectively] the curves have a rather simple form which has a peak at $\theta \approx 90°$ and is nearly symmetric about it. For π^+ there is agreement[49-51] beyond $\theta \gtrsim 30°$, the discrepancy in the forward direction being due to t-channel effects which decline rapidly beyond about 10°. The same is true for π^- except for somewhat lower accuracy of the data. On the whole, the angular distribution conforms to our theoretical expectations. To get a more precise significance of the various reso-

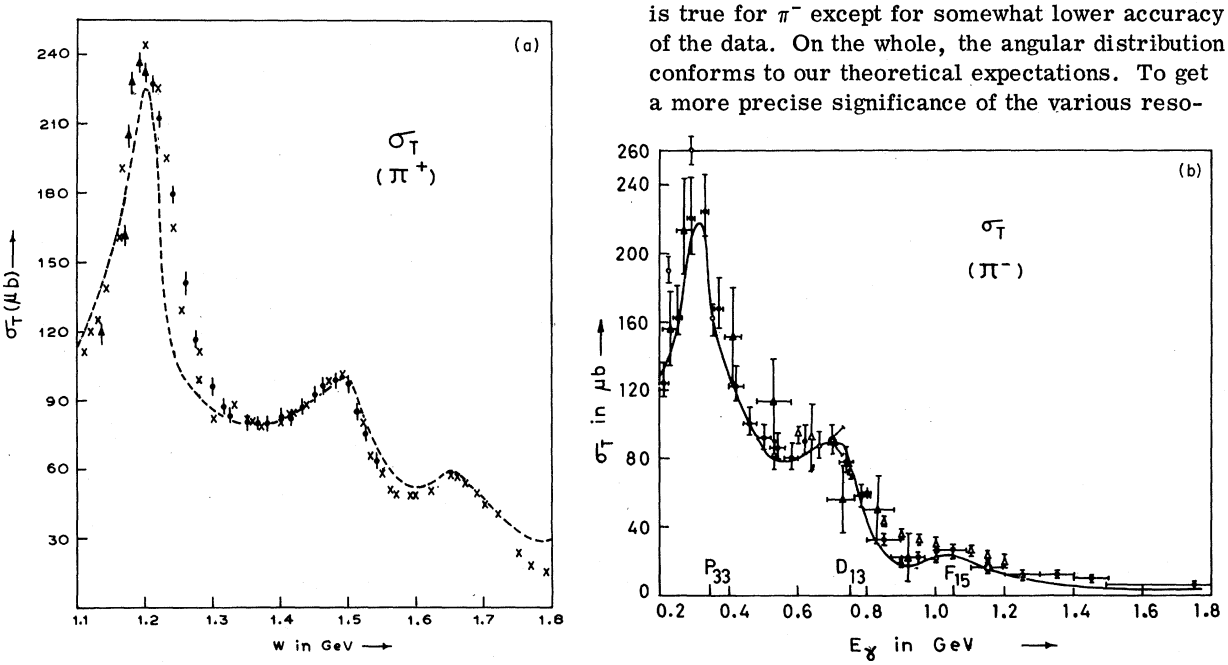

FIG. 3. (a) Total cross section with "old" form factor for the process $\gamma p \to \pi^+ n$ as a function of total c.m. energy E_γ in GeV compared with the data of (●) Ref. 32; (▲) Ref. 33; and (×) Ref. 34 and Ref. 21. (b) Total cross section with "new" form factor for the process $\gamma n \to \pi^- p$ as a function of E_γ compared with the data of (●) Ref. 35; (○) Ref. 36; (×) Ref. 37; (▲) Ref. 38; and (△) Ref. 39.

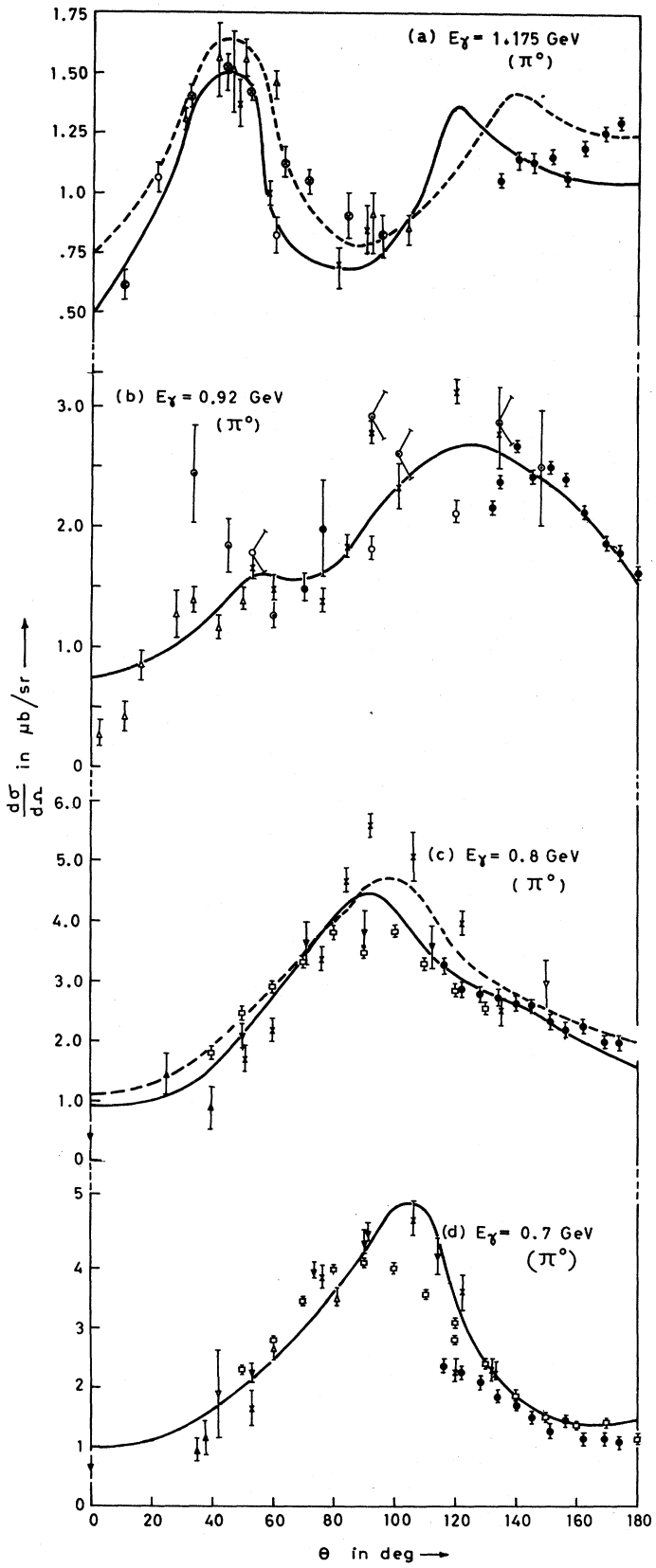

Fig. 4. Differential cross section $d\sigma/d\Omega$ in μb/sr for π^0 process as a function of pion-nucleon c.m. angle θ in deg at the fixed lab photon energies indicated, compared with the following experimental data:

(×) Ref. 30; (▼) Ref. 42; (▲) Ref. 46;
(□) Ref. 31; (⧗) Ref. 43; (▽) Ref. 47;
(●) Ref. 40; (○) Ref. 44; (⊗) Ref. 48.
(△) Ref. 41; (⊙) Ref. 45;

The Orsay data (Ref. 40) in both (a) and (b) are at $E_\gamma = 1.15$ GeV and $E_\gamma = 0.90$ GeV, respectively. The solid and dashed curves are with the "new" and "old" form factors, respectively.

nance contributions to these angular distributions, it is necessary to make a partial-wave analysis on the lines of Walker.[15] However, since our fits to the data for the cases considered are almost as good as Walker's[15] (not shown in the figures) except for t-channel contributions, this part of the discussion would be essentially the same as in Walker's analysis.

We now come to the more interesting question of the energy distribution of differential cross sections at fixed angles, which should indicate how the capacity (or lack of it) of a particular resonance to show up at the appropriate energy varies with angle. This question, which has a bearing on the experimental features (a) and (b) listed in the beginning of this section, is closely related to the features of the particular theoretical model one is considering. For example, in the quark model of CKO the lack of contribution of F_{15} in backward direction is ascribed to a cancellation between the spin and orbital contributions to the helicity amplitude $A_{1/2}$ for the π^0 and π^+ processes, while the other helicity amplitude $A_{3/2}$ does not contribute in the backward direction. In our model the corresponding terms in the interaction are represented by magnetic [type (A)] and minimal [type (B)], proportional to charge, respectively. Specifically, the respective counterparts of the two CKO spin and orbital terms R^{λ}_{L0} and R^{λ}_{L1}, respectively, in our model, apart from irrelevant factors, are given by

$$A\left(\tfrac{5}{3}\tau_3+\hat{1}\frac{1}{3}\frac{m_\omega}{m_\rho}\right)\frac{e}{g_\rho}m_\rho{}^2 \tag{5.1}$$

and

$$B\left(\tau_3+\hat{1}\frac{m_\omega}{m_\rho}\right)\frac{e}{g_\rho}m_\rho{}^2, \tag{5.2}$$

respectively. Similarly, the selection rule of CKO, which says that the $A_{3/2}$ helicity amplitude vanishes identically for photoexcitation off neutrons of $I=\frac{1}{2}$ resonances belonging to $\underline{56}$ (a result borne out by recent experiment[39]), is seen to be automatically satisfied in our model, where the minimal-coupling term represented by Eq. (5.2) vanishes for neutrons. Note that the selection rule is violated in our model of vector dominance only to the extent that $m_\rho \neq m_\omega$; on the other hand, our

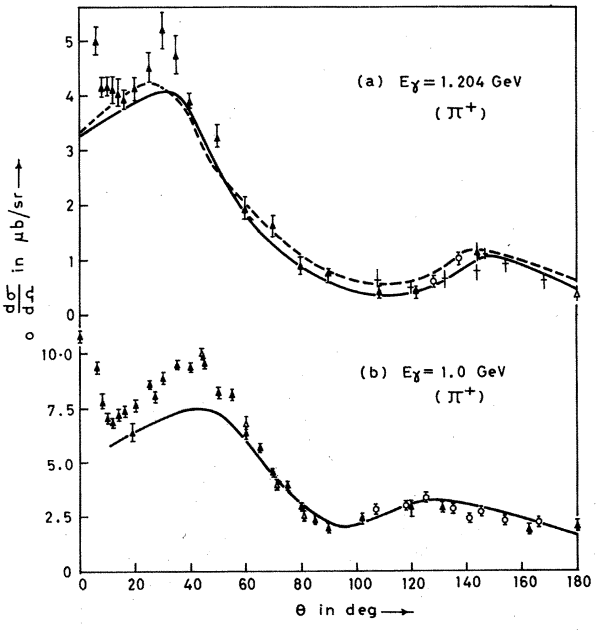

FIG. 5. Differential cross section for π^+ process as a function of θ at fixed values of E_γ indicated, compared with the experimental data of (▲) Ref. 21; (△) Ref. 49; (○) Ref. 50; and (–) Ref. 51.

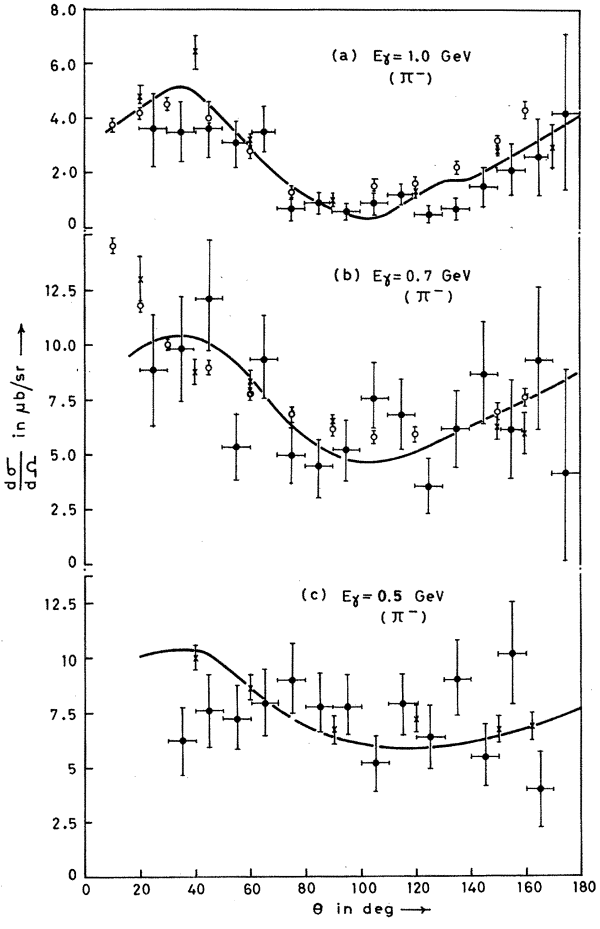

FIG. 6. Differential cross section for π^- process as a function of θ at fixed values of E_γ compared with the data of (●) Ref. 35; (○) Ref. 39; and (×) Ref. 36. The data of Ref. 35 are at $E_\gamma = 0.95\pm0.05$, 0.7 ± 0.02, and 0.5 ± 0.02 GeV in (a), (b), and (c), respectively.

model does not have a separate $L\cdot S$ term, which, as CKO point out, would lead to an independent violation of their selection rule.

To discuss the more quantitative details of the prediction between the theory and experiment we now turn to Figs. 7, 8, and 9 which display the energy distribution of the process π^0, π^+, and π^- at the angles 45°, 90°, 135°, 140°, 150°, and 180°. For completeness we also show the curve for π^0 [Fig. 7(a)] in the forward direction, as this case is free from t-channel effects. From this curve we notice the absence of D_{13} and F_{15} in agreement with experimental data. As a matter of fact this curve shows no peak other than the P_{33}. In the backward direction the π^0 curves are shown for both types of form factors against experimental data. The new form factor which gives slightly lower values as compared to the "old" form factor seems to agree with the more recent Cornell data, [52] while the curves with the old form factor happen to give good overlap with Orsay data.[40] Further, the peaks appear to be somewhat sharper with the "new" form factor rather than the "old". In the absence of an independent judgment on the relative qualities of Orsay and Cornell data, it is not possible to make any further comments on these features.

A comparison with experimental data of the curves for π^0 and π^+ [Figs. 7(d) and 8(d)] in the backward direction shows again the absence of the D_{13} and F_{15} peaks. Presumably, this feature is a result of cancellation of the right magnitudes between the magnetic and minimal terms [of the types (A) and (B)] though no adjustment of parameters is involved in this model unlike the quark model of CKO. The Δ resonances P_{33} and F_{37} are seen to show up quite prominently in the backward direction, in agreement with the experimental points. At the same time the other Δ resonances, viz., S_{31} and D_{33}, do not seem to show up, a result which again is not in discord with the data. The quark-model explanation of this fact is simply that the positive-parity Δ's belonging to $\underline{56}$ have quark spin $S=\frac{3}{2}$, while negative-parity Δ's belonging to $\underline{70}$ have $S=\frac{1}{2}$. As explained by CKO, this property of the $\underline{56}$ Δ's excludes any contribution to the amplitude arising from the "charge" term [in our language the "minimal" coupling (52)], thus leaving no possibility of cancellation in the total amplitude due to such Δ exchanges. However, for $\underline{70}$ Δ's of $S=\frac{1}{2}$ both charge and magnetic terms contribute (though only via the ρ term) so that there is now a bigger possibility of "smearing out" of their respective effects. In our model which makes use of all the basic qualitative features of the quark model the same property is automatically present in the $V\bar{B}B_L$ couplings, via vector dominance, so that only the $\underline{56}$ Δ's show up prominently, while the $\underline{70}$ Δ's do not.

Finally, we give a brief description of the energy distribution of the differential cross section at intermediate angles (45°, 90°, 135°, 140°, 150°) for the three different cases as shown in Figs. 7, 8, and 9. The most prominent contributor is P_{33}, which shows up uniformly at all angles. However, its Regge recurrence F_{37} seems to be prominent at 180° and declines at other angles rapidly. The effect of D_{13} builds up from near zero at 180° to maximum in the angular range 135° to 90°, below which it starts to decline. F_{15} shows a similar trend (though less prominently), its maximum arising in the somewhat lower angular range. There do not seem to be any more striking features for the other resonances. The qualitative features of π^0 and π^+ are very similar at these angles, while for π^- much less structure seems to be visible, though this fact has to be seen in the context of less accurate data.

Our theoretical curves, most of which have been drawn with the "new" form factor, compare quite well with the experimental points in general and the above trends in particular. The cross section data do not seem to be very sensitive to the difference in the "new" and "old" form factors, but the electromagnetic decay widths obtained with the latter are appreciably higher than the former. This can probably be understood in the following manner. Firstly, it is seen from the calculations that the $L=0$ resonances, viz., $N(938)$, $N(1470)$, and $\Delta(1238)$, give the most significant contributions to the cross section, and for these states there is no difference between the "old" and "new" form factors. Secondly, although the electromagnetic decay widths with the "new" form factor are much lower than with the "old" one, the $B_L \to BP$ decays are not much different. Lastly, we presume that since with the two form factors there is no change in the sign of any resonant amplitude, the cancellation patterns arising from them for the two cases are similar. Also, there seems to be a good deal of "scatter" in the experimental data of different groups.

Since we have made a single-channel calculation our theorectical curves do not contain features like η-threshold effects,[15,19,53] which are expected to manifest themselves as cusps near the appropriate energy region. Experimentally this feature seems to be barely visible in the π^0 case at $k=0.72$ GeV corresponding to η threshold. However since it is not a prominent effect, we prefer not to discuss this point any further. On the whole our theoretical curves agree quite well with the data in sufficient detail.

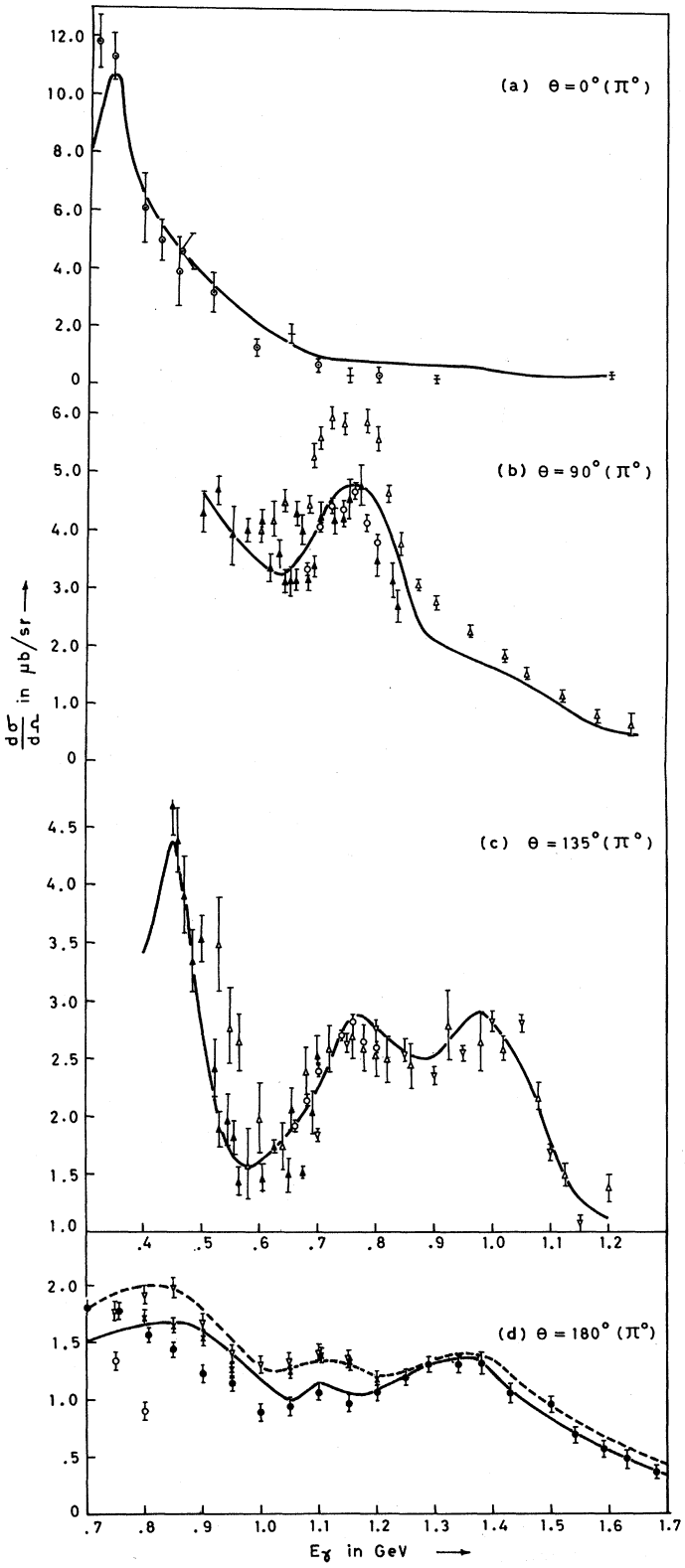

FIG. 7. Differential cross section for π^0 process as a function of E_γ at the fixed indicated values of θ compared with the following experimental data:

(×) Ref. 29; (△) Ref. 40; (●) Ref. 52;
(△) Ref. 30; (–) Ref. 41; (▲) Ref. 53.
(○) Ref. 31; (○) Ref. 43;

In (a) the data of Ref. 41 are at $\theta \approx 5°$, in (b) the data of Ref. 30 are at $\theta \approx 92°$, and in (c) the data of Refs. 31 and 40 are at $\theta \approx 130°$ and $\theta \approx 134°$, respectively.

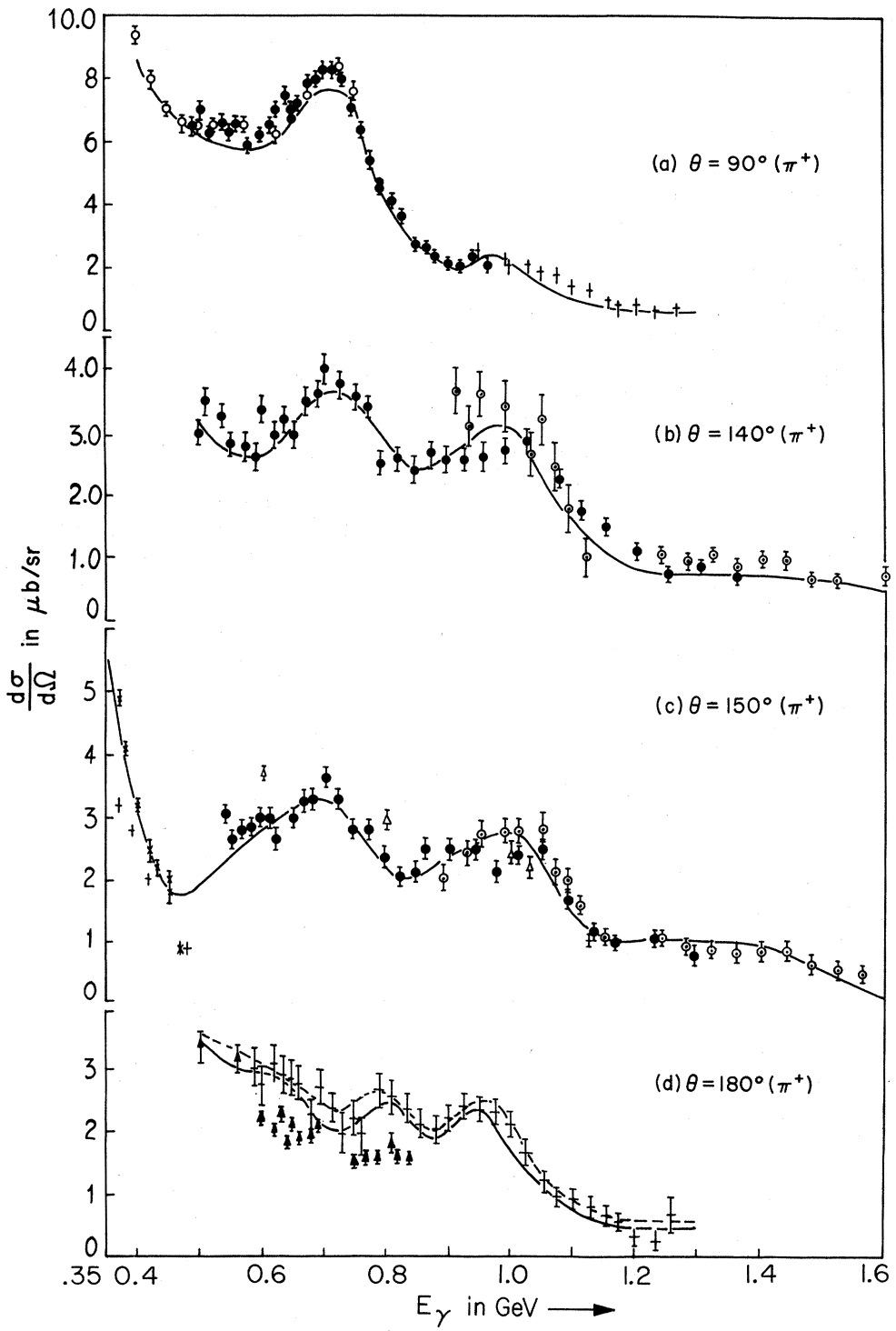

FIG. 8. Differential cross section for π^+ process as a function of E_γ at the fixed values of θ indicated, compared with the following experimental data:

(○) Ref. 32; (△) Ref. 49; (●) Ref. 50; (⊙) Ref. 54;
(▲) Ref. 55; (×) Ref. 56; (–) Ref. 21 and Ref. 57.

The experimental data of Thiessen *et al.* (Ref. 50) are at c.m. angles $\theta = (90 \pm 5)°$, $(143 + 5)°$, $(153 + 3)°$ in (a), (b), and (c), respectively, and the data of Alvarez *et al.* (Ref. 54) are at $\theta = (140 \pm 4)°$ and $(151 \pm 3)°$ for (b) and (c), respectively.

D. Recoil-Proton Polarization

Finally, we have calculated the energy dependence of the polarization, $P(\theta)$, of the recoil proton in the reaction $\gamma p \to \pi^0 p$. The results are shown in Figs. 10(a) and 10(b) corresponding to $\theta = 60°$ and 90°, respectively, together with the experimental data[58-64] (which are predominantly negative). In this calculation only the "new" form factor has been used, since the results for $P(\theta)$ are fairly insensitive to the actual magnitudes of the couplings and depend more on their kinematical (i.e., spin and angular dependent) structures. The polarization experiments are of interest since they show the interference between different-parity states.[19,60] In particular, an appreciable value of $|P(\theta)|$ in any region is expected to indicate the presence of two interfering states with opposite parity, while a small value is supposed to be a signal for interference between like-parity states.[60] The main experimental features of a prominent peak in $|P(\theta)|$ near $E_\gamma \sim 0.7$ GeV and a much smaller magnitude for the same quantity near $E_\gamma \sim 0.9$ GeV are seen to be well reproduced by the theoretical curves [which of course agree on the sign of $P(\theta)$]. According to Sakurai[65] the peak in $|P(\theta)|$ [i.e., dip in $P(\theta)$, algebraically] is a result of interference between the opposite-parity states P_{33} and $D_{13}(1515)$. As we have already seen earlier in this section, in connection with the total and differential cross sections, these two resonances play an important role in reproducing many experimental features. Our result for $P(\theta)$ also seems to bring out quite well Sakurai's conjecture[65] on the relative roles of the D_{13} and P_{33} states with regard to the polarization feature at $E_\gamma \sim 0.7$ GeV. As for the near-zero value of $P(\theta)$ in the region $E_\gamma \sim 0.9$ GeV, a reasonable interpretation is that it is due to the interference of a few important negative-parity states which happen to be in that

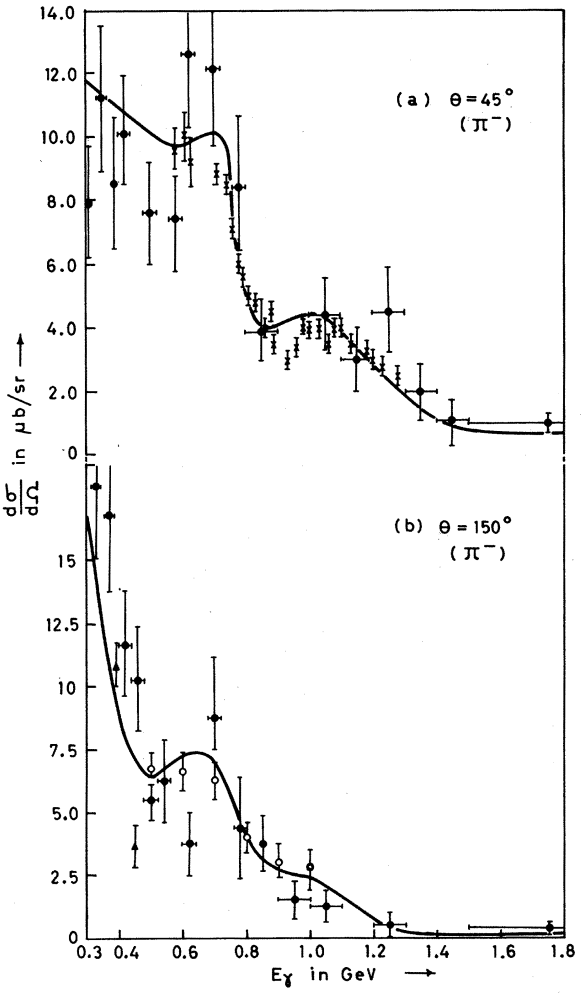

FIG. 9. Differential cross section for π^- process as a function of E_γ at the fixed values of θ indicated, compared with the following experiments:

(●) Ref. 35; (○) Ref. 36; (×) Ref. 39; and (▲) Ref. 37. The data of Ref. 35 are at $\theta = (145 \pm 5)°$ and $(45 \pm 5)°$ in (b) and (a), respectively.

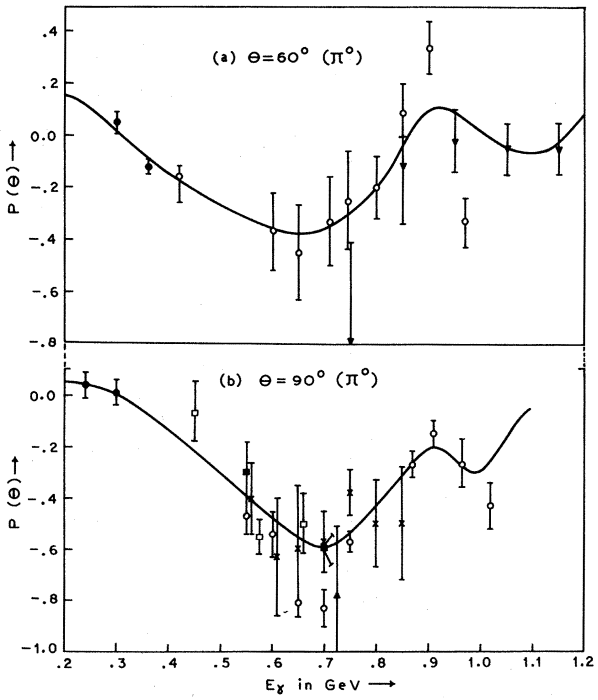

FIG. 10. Polarization $P(\theta)$ of the recoil proton in the reaction $\gamma p \to \pi^0 p$ as a function of E_γ at the indicated values of θ compared with the following experimental data:

(○) Ref. 58; (●) Ref. 59; (×) Ref. 60; (▲) Ref. 61; (□) Ref. 62; (■) Ref. 63; (▼) Ref. 64.

region, the most likely candidates according to our model being the d-state resonances $D_{13}(1520)$ and $D_{33}(1670)$ rather than the s-state resonances $S_{11}(1525)$ and $S_{31}(1630)$, which according to our results on differential cross section contribute much less to the $\gamma N \to \pi N$ process.[66]

VI. SUMMARY AND CONCLUSIONS

We have investigated pion photoproduction off nucleons via s-channel resonances, as well as the electromagnetic decay widths of these resonances, using a model of $\overline{B}B_L P$ and $\overline{B}B_L V$ interactions based on the following ingredients:

(i) The quark model is used as a guide to the evaluation of relativistic $\overline{B}B_L P$ couplings of baryon resonances, which in turn are classified according to the $(\underline{56}, 2L^+)$ and $(\underline{70}, (2L+1)^-)$ representations of SU(6)×O(3). These couplings are expressed in a multiple-derivative form together with a relativistic (though phenomenological) form factor governing the entire supermultiplet transition $(L^P \to 0^+)$.

(ii) Partial symmetry is used for relating the structures of both $\overline{B}B_L P$ and $\overline{B}B_L V$ couplings in a unified framework so that the same form factor can be used for both.

(iii) VDM is employed for obtaining the couplings of the $\overline{B}B_L$ currents to the electromagnetic field via ρ and ω mesons.

This model makes use of much fewer parameters than, e.g., similar calculations based on the more conventional quark model,[1,2] or a partial-wave analysis[15] where several parameters must be "determined" through the use of suitable experimental constraints. The study is confined to the intermediate-energy region (1–2 GeV) which includes all the resonances of $L=0$, 1, 2 in the above classification. We do not consider the lower-energy region ($W<1.2$ GeV) for which excellent treatments already exist in terms of dispersion theory,[67] nor do we consider the much-higher-energy region which is more economically described in the Regge formalism. However, in this limited energy range we have tried to explore the possibilities of noticing "duality" effects by comparing our results with experimental data in the forward and backward directions. Thus in the backward direction our results agree quite well with the experimental points without the inclusion of a separate u-channel effect. On the other hand, in the near forward direction our numbers fall considerably short of the experimental data, yet the ratio of the π^+ to π^0 cross sections is appreciably larger than what would be expected simply from considerations of isospin effects, thus leading to the conclusion that the t-channel pion exchange is presumably simulated, at least in a partial manner, through the s-channel mechanism provided by our limited list of resonances. Our model automatically exhibits the features leading to the Moorhouse selection rule[20] for $S=\frac{3}{2}$ resonances and the CKO "charge" selection rule for $\underline{56}$ states of $I=\frac{1}{2}$ resonances, in the limit where the mass difference between ρ and ω mesons is neglected.

The calculations which have been done with the two types of form factors (2.2) and (2.3), termed "old" and "new," respectively, not only exhibit the main experimental features with respect to the prominent resonances D_{13}, F_{15}, and some $\underline{56}$ Δ's, but give quite a detailed quantitative fit to the experimental curves for π^0, π^+, and π^- photoproduction. These curves include the following types of data: (i) total cross section, (ii) angular distribution of differential cross section at different energies, (iii) energy distribution of differential cross section at different angles, and (iv) recoil-proton polarization. From these data on photoproduction it is difficult to distinguish between the effect of the two form factors, both of which seem to fit the data fairly well, though on the whole the resonance structures are found to be somewhat sharper with the new form factor. Reasons for this insensitivity of the photoproduction cross sections to the form factors have been discussed in Sec. V. A greater sensitivity to the structure of the two form factors seems to be afforded by the electromagnetic decay widths, for which the "old" form factor predicts appreciably higher magnitudes than the "new" form factor. However in the absence of much experimental data on radiative decay widths a direct test of this difference is not yet possible. The comparison therefore has to be limited to the predictions of other types of investigations, especially the quark model[1,2] and multipole analyses of photoproduction data,[19] which seem to exhibit fairly good overlaps with the predictions of the "new" form factor. The only available experimental data are on the resonances P_{33} and Λ_{03} for which our model with the "new" form factor gives excellent answers.

Before we conclude, it is useful to add some remarks about the problem of gauge invariance in our model. It might appear at first sight that this property is being violated for the nucleon Born term, since we have not included the pion-exchange term (for $\pi^\pm$ production) and the u-channel nucleon Born term (for $\pi^\pm$ production) over and above the s-channel nucleon effect. But then a natural question that arises concerns the possible u-channel effects of the higher resonances. Should each resonance be included in both s and u channels to ensure proper gauge invariance? But

then one cannot be sure if such a procedure does not amount to violating the spirit of "strong" duality, which we are more interested in exploring in this paper than, e.g., an interference model. While it is desirable, almost mandatory, to preserve gauge invariance explicitly, there does not yet appear to exist a model-independent way of ensuring this in a phenomenological model.[68] On the other hand, the *ad hoc* prescription of adding all the resonances in the u channel together with their s-channel effects (as one would do for a nucleon pole) is too high a price to pay for gauge invariance within our approach, since in our model the nucleon is merely one of a series of "poles." A possible way out of this dilemma, at a time when there exists no foolproof guideline for constructing dual amplitudes for meson-baryon or photoproduction processes, is the following point of view that we take in this paper. Let us for the moment believe in the usual "folklore" that s-channel amplitudes are not to be duplicated with contributions from other channels if duality is to make sense. As for the gauge-invariance problem, we are forced to pretend that the inclusion of the higher resonances in the s-channel probably "simulates" the effect of the u-channel nucleon pole, though we cannot substantiate this point in any theoretical manner.[68] For the t-channel pion pole, the problem is still more complicated, and for this reason we have already recognized the futility of comparison of $\pi^{\pm}$ production data for $\theta \lesssim 10°$ to 15°. The same limitation also applies to Coulomb effects which are well within this θ region.

On the whole our model seems to work reasonably well in the intermediate-energy region. While it is possible in principle to extend this analysis to a higher-energy region through the inclusion of still higher resonances, the experimental pattern for the latter does not seem to be clear except for a few Δ-type states, so that such an analysis will be necessarily incomplete without the use of further theoretical principles.

A similar procedure can be employed for the photoproduction of other types of states like $K\Lambda$, $K\Sigma$, ηN, and $X_0 N$. In particular, the evaluation of η photoproduction cross sections, for which enough data are available in this energy region, is currently in progress, and the results will be reported in a separate communication.

ACKNOWLEDGMENTS

We are extremely indebted to Dr. (Mrs.) S. Sen (neé Das Gupta), who was closely associated with the early stages of this investigation and gave us invaluable help by way of various discussions in the subsequent steps, as well. We are also very grateful to Professor S. H. Patil, Dr. D. K. Choudhury, and Miss K. Sen Gupta for various enlightening discussions. One of us (RM) gratefully acknowledges a Research Fellowship from the Council of Scientific and Industrial Research.

[1]L. A. Copley, G. Karl, and E. Obryk, Nucl. Phys. B13, 303 (1969), referred to as CKO in text.
[2]D. Faiman and A. W. Hendry, Phys. Rev. 180, 1572 (1969).
[3]K. C. Bowler, Phys. Rev. D 1, 926 (1970).
[4]A. N. Mitra, Nuovo Cimento 61A, 344 (1969); 64A, 603 (1969).
[5]A. N. Mitra, in *Lectures in High Energy Theoretical Physics*, edited by H. H. Aly (Gordon and Breach, London, 1970).
[6]K. T. Mahanthappa and E. C. G. Sudarshan, Phys. Rev. Letters 14, 163 (1965).
[7]A. N. Mitra, Nuovo Cimento 56A, 1164 (1968).
[8]O. W. Greenberg, Phys. Rev.Letters 13, 598 (1964).
[9]R. H. Dalitz, in *Conference on πN Scattering, Irvine, California, 1967*, edited by G. L. Shaw and D. Y. Wong (Wiley, New York, 1967).
[10]H. Harari, rapporteur talk on resonances, in *Proceedings of the Fourteenth International Conference on High Energy Physics, Vienna, 1968*, edited by J. Prentki and J. Steinberger (CERN, Geneva, Switzerland, 1968).
[11]J. Schwinger, Phys. Rev. Letters 18, 923 (1967).
[12]R. Dashen, Phys. Rev. 183, 1245 (1969).
[13]J. J. Sakurai, Ann. Phys. (N.Y.) 11, 1 (1960); M. Gell-Mann, Phys. Rev. 125, 1067 (1962).
[14]G. F. Chew, M. L. Goldberger, F. E. Low, and Y. Nambu, Phys. Rev. 106, 1345 (1957).
[15]R. L. Walker, Phys. Rev. 182, 1729 (1969).
[16]A. N. Mitra, Ann. Phys (N.Y.) (to be published).
[17]D. K. Choudhury and A. N. Mitra, Phys. Letters 32B, 619 (1970).
[18]D. L. Katyal and A. N. Mitra, Phys. Rev. D 1, 338 (1970).
[19]Y. C. Chau, N. Dombey, and R. G. Moorhouse, Phys. Rev. 163, 1632 (1967); R. G. Moorhouse and W. A. Rankin, Nucl. Phys. B23, 181 (1970).
[20]R. G. Moorhouse, Phys. Rev. Letters 16, 772 (1966).
[21]S. D. Ecklund and R. L. Walker, Phys. Rev. 159, 1195 (1967).
[22]R. H. Dalitz and D. G. Sutherland, Phys. Rev. 146, 1180 (1966).
[23]T. S. Mast, M. Alston-Garnjost, R. O. Bangerter, A. Barbaro-Galtieri, L. K. Gershwin, F. T. Solmitz, and R. D. Tripp, Phys. Rev. Letters 21, 1715 (1968).
[24]A. Donnachie, Phys. Letters 24B, 420 (1967); see, however, F. A. Berends and A. Donnachie, *ibid.* 30B, 555 (1969).
[25]G. Schwiderski, thesis, Karlsruhe University, 1967 (unpublished).
[26]C. Fronsdal, Suppl. Nuovo Cimento 9, 416 (1958);

R. Blankenbecler and R. L. Sugar, Phys. Rev. 168, 1597 (1968).
[27]K. Sen Gupta and V. K. Gupta, following paper, Phys. Rev. D 5, 1824 (1972).
[28]D. S. Beder, Nuovo Cimento 33, 94 (1964).
[29]G. Buschorn, P. Heide, U. Kötz, R. A. Lewis, P. Schmüser, and H. J. Skromm, Phys. Rev. Letters 20, 230 (1968).
[30]C. Ward, B. Kenton, and C. York, Phys. Rev. 159, 1176 (1967).
[31]H. De Staebler, E. F. Erickson, A. C. Hearn, and C. Schaerf, Phys. Rev. 140, B336 (1965).
[32]C. Betourne, J. C. Bizot, J. Perez-Y-Jorba, D. Trielle, and W. Schmidt, Phys. Rev. 172, 1343 (1968).
[33]D. Freytag, W. J. Schwille, and R. J. Wedemeyer, Z. Physik 186, 1 (1965).
[34]J. T. Beale, S. D. Ecklund, and R. L. Walker, Cal. Tech. Report No. CTSL-42, 1966 (unpublished).
[35]Aachen, Berlin, Bonn, Hamburg, Heidelberg, München Collaboration, Nucl. Phys. B8, 535 (1968).
[36]G. Neugebauer, W. Wales, and R. L. Walker, Phys. Rev. 119, 1726 (1960).
[37]M. Sands, J. G. Teasdale, and R. L. Walker, Phys. Rev. 95, 592 (1954).
[38]D. H. White, R. M. Schectman, and B. M. Chasan, Phys. Rev. 120, 614 (1960).
[39]P. E. Scheffler and P. L. Walden, Phys. Rev. Letters 24, 952 (1970).
[40]B. Delcourt, J. Lefrancois, G. Parrour, J. P. Perez-Y-Jorba, and G. Sauvage, Phys. Letters 29B, 71 (1969).
[41]R. M. Talman, C. R. Clinesmith, R. Gomez, and A. V. Tollestrup, Phys. Rev. Letters 9, 177 (1962).
[42]R. M. Worlock, Phys. Rev. 117, 537 (1960).
[43]V. L. Highland and J. W. DeWire, Phys. Rev. 132, 1293 (1963).
[44]R. Diebold, Phys. Rev. 130, 2089 (1963).
[45]J. I. Vette, Phys. Rev. 111, 622 (1938).
[46]Karl Berkelman and J. A. Waggoner, Phys. Rev. 117, 1364 (1960).
[47]G. Bellettini, C. Bemporad, P. J. Biggs, and P. L. Braccini, Nuovo Cimento 44, 239 (1966).
[48]C. R. Clinesmith, G. L. Hatch, and A. V. Tollestrup, in *International Symposium on Electron and Photon Interactions at High Energies, Hamburg, 1965* (Springer, Berlin, 1966), Vol. II, p. 245.
[49]F. P. Dixon and R. L. Walker, Phys. Rev. Letters 1, 142 (1958).
[50]H. A. Thiessen, Phys. Rev. 155, 1488 (1967).
[51]J. R. Kilner, Ph.D. thesis, Caltech, 1963 (unpublished).
[52]G. L. Cassiday, H. Fisher, A. Ito, E. C. Loh, and J. Rutherford, Phys. Rev. Letters 21, 933 (1968).
[53]C. Bacci, G. Penso, G. Salvini, C. Mencuccini, A. Reale, V. Silvestrini, M. Spinetti, and B. Stella, Phys. Rev. 159, 1124 (1967).
[54]R. A. Alvarez, G. Cooperstein, K. Kalata, R. C. Lanza, and D. Luckey, Phys. Rev. D 1, 1946 (1970).
[55]C. Schaerf, Nuovo Cimento 44, 504 (1966); L. Hand and C. Schaerf, Phys. Rev. Letters 6, 229 (1961).
[56]A. V. Tollestrup, J. C. Keck, and R. M. Worlock Phys. Rev. 99, 220 (1955).
[57]R. L. Walker, J. G. Teasdale, V. Z. Peterson, and J. J. Vette, Phys. Rev. 99, 210 (1955).
[58]D. E. Lundquist, R. L. Anderson, J. V. Allaby, and D. M. Ritson, Phys. Rev. 168, 1527 (1968).
[59]K. H. Althoff, D. Finken, N. Minatti, H. Piel, D. Trines, and M. Unger, in *Proceedings of the Third International Symposium on Electron and Photon Interactions at High Energies, Stanford Linear Accelerator Center, Stanford, California, 1967* (Clearing House of Federal Scientific and Technical Information, Washington, D.C., 1968), p. 593.
[60]R. Querzoli, G. Salvini, and A. Silverman, Nuovo Cimento 19, 53 (1961).
[61]L. Bertanza, P. Franzini, I. Mannelli, and G. V. Silvestrini, Nuovo Cimento 19, 953 (1961).
[62]J. O. Malov, G. A. Salandin, A. Manfredini, V. Z. Peterson, J. I. Friedman, and H. Kendall, Phys. Rev. 122, 1338 (1961).
[63]P. C. Stein, Phys. Rev. Letters 2, 473 (1959).
[64]E. Bloom, C. Heusch, C. Prescott, and L. Rochester, Phys. Rev. Letters 19, 671 (1967).
[65]J. J. Sakurai, Phys. Rev. Letters 1, 258 (1958).
[66]This conclusion seems to be somewhat at variance with that of Ref. 58 who find a more important role for the $S_{11}(1535)$ state.
[67]J. Engels, G. Schwiderski, and W. Schmidt, Phys. Rev. 166, 1343 (1968); F. A. Berends, A. Donnachie, and D. L. Weaver, Nucl. Phys. B4, 54 (1967); A. Donnachie and G. Shaw, Ann. Phys. (N.Y.) 37, 333 (1966).
[68]Another possibility which preserves explicit gauge invariance is to take a less restrictive view of duality and add all the u-channel resonance contributions, since, after all, only the *real part* of the amplitude would be affected in that way. We are, however, more interested in exploring the possibilities of "strong" duality, where even the real part is hopefully simulated. It appears from the numerical results in retrospect that perhaps the u-channel contributions are not significant, so that the problem of gauge invariance in this context is more academic than physical.